Characterization of Site-Directed Mutants in the Cytochrome c-550 Protein of Photosystem II

by

Akarsh Manne

August, 2010

Chair: Jeff McKinnon

Major Department: Biology

Photosynthesis is the process by which cyanobacteria, algae, and higher plants convert light energy to chemical energy via the biosynthesis of carbohydrates. Photosystem II is a multi-protein/pigment complex embedded in the thylakoid membrane. CP43 is the product of the *psbC* gene, and is an intrinsic component of the photosystem II complex. CP43 is 473 amino acids long and has five hydrophilic loops connecting six transmembrane alpha helices, including a large extrinsic loop E which is exposed to the lumenal side of the thylakoid membrane. Short deletions of regions of the loop E of CP43 resulted in mutants that fail to grow photoautotrophically and are devoid of oxygen-evolving activity. A mutation was introduced in loop E that altered arginine at position 305 to a serine residue, producing a mutant with severely reduced growth and oxygen evolving activity under chloride limiting conditions. However, when grown under normal conditions, the R305S mutant showed no extreme phenotype. After isolation of photosystem II particles and chemilumininescent staining for cytochromes, it was determined that this specific mutation resulted in loss of binding of an extrinsic photosystem II protein, cytochrome c-550. Deletion of the *psbV* gene encoding cytochrome c-550 resulted in the loss of photoautotrophic growth in media lacking chloride and/or calcium. X-ray crystallography of photosystem II does in fact show a close proximity between cytochrome c-550 and CP43. Based on the crystal structure, two residues on cytochrome c-550 were identified

that might interact with CP43 and are in close proximity with the arginine residue at position 305. These residues on cytochrome c-550 are both highly conserved asparagines, located at positions forty nine and fifty one. In this work, the asparagine residue at position fifty one on cytochrome c-550 was mutated to either an alanine or aspartic acid residue. The N51 mutations were transformed into wildtype *Synechocystis*, a cyanobacterial model organism that has been widely used to study photosystem II. The N51 mutants were characterized by photoautotrophic growth in complete and chloride-limiting media, oxygen evolution assays, variable florescence yield measurements and photoinactivation assays. Based on these assays, the control and N51 mutant strains exhibited similar phenotypes in complete media while the control and N51D mutant strains exhibited similar phenotypes in chloride limiting media. The N51A mutant had a small but reproducible decrease in photoautotrophic growth rate, oxygen evolution rates and enhanced sensitivity to photoinactivation in chloride limiting media. Therefore, asparagine at position fifty one on cytochrome c-550 might contribute to a weak interaction between arginine on CP43 and cytochrome c-550, which is likely to involve hydrogen bonding. However, further studies are needed to validate the proposed interaction between subunits cytochrome c-550 and CP43 of photosystem II.

Characterization of Site-Directed Mutants in the Cytochrome c-550 Protein of Photosystem II

A Thesis

Presented To

The Faculty of the Department of Biology

East Carolina University

In Partial Fulfillment

of the Requirements for the Degree

Master of Science in Molecular Biology/Biotechnology

by

Akarsh Manne

August, 2010

CHARACTERIZATION OF SITE-DIRECTED MUTANTS IN THE CYTOCHROME c-550 PROTEIN OF PHOTOSYSTEM II

by

Akarsh Manne

APPROVED BY:

DIRECTOR OF THESIS: _____
(Cindy Putnam-Evans, PhD)

COMMITTEE MEMBER: _____
(Colin Burns, PhD)

COMMITTEE MEMBER: _____
(Paul Hager, PhD)

COMMITTEE MEMBER: _____
(Jean-Luc Scemama, PhD)

CHAIR OF THE DEPARTMENT OF BIOLOGY: _____
(Jeff McKinnon, PhD)

DEAN OF THE GRADUATE SCHOOL: _____
(Paul J. Gemperline, PhD)

DEDICATION

I dedicate this thesis to my family.

ACKNOWLEDGEMENTS

I would like to thank my advisor Dr. Cindy Putnam-Evans for providing guidance and support throughout my research. My sincere thanks go to Dr. Paul Hager for all his insights and the numerous ways he contributed to my project. I would like to thank Dr. Jean-Luc Scemama and Dr. Colin Burns for serving on my thesis committee and their insightful comments. I am grateful to Denise Mayer for always taking the time to answer my questions and Ethan Dunn who initially guided and trained me.

Last but not least, I would like to thank my family: my parents Lakshmana and Lakshmi Manne, and my sister and brother-in-law Sravanthi and Sreekanth Chinta.

TABLE OF CONTENTS

LIST OF FIGURES

LIST OF TABLES

LIST OF ABBREVIATIONS

Å: Ångströms

ADP: Adenosine diphosphate

ATP: Adenosine triphosphate

CTAB: Cetyl trimethylammonium bromide

Cyt b_6f: Cytochrome b_6f complex

Cyt c-550: Cytochrome c-550

DCBQ: 2,5- dichloro-1,4-benzoquinone

DCMU: 3-(3,4-dichlorophenyl)-1,1-dimethylurea

EDTA: Ethylenediaminetetraacetic acid

Fd: Ferredoxin

FNR: Ferredoxin-NADP(H)-oxidoreductase

MSP: Manganese stabilizing protein

PCR: Polymerase chain reaction

PSI: Photosystem I

PSII: Photosystem II

RPM: Revolutions per minute

CHAPTER 1: INTRODUCTION

Photosynthesis

Photosynthesis is a critical metabolic pathway carried out by green plants, algae and cyanobacteria, that produces essentially all of the oxygen in earth's atmosphere. During photosynthesis, diatomic oxygen is released into the atmosphere while carbon dioxide is reduced to form simple sugars in a series of anabolic reactions. Photosynthesis is divided into two sets of reactions: light-dependent reactions and light-independent (dark) reactions. Diatomic oxygen is evolved following the splitting of water molecules during the light-dependent reactions, while simple sugars are synthesized via the Calvin cycle during light-independent reactions.

The light-dependent reactions take place within a number of membrane bound complexes in the thylakoid membrane: light-harvesting antennas, photosystem II (PSII), cytochrome b_6f complex (Cyt b_6f), photosystem I (PSI) and ATPase. Thylakoid membranes are tube-like structures; volume inside the membrane is the lumen and volume outside the membrane is referred to as the stroma (cytoplasm in cyanobacteria) (Campbell et al., 1998). Water-splitting and oxygen evolution occur on the lumenal face of the thylakoid, while the Calvin cycle reactions occur in the stroma.

The light-harvesting antennas in cyanobacteria are usually phycobilisomes, extrinsic light absorbing complexes that transfer light energy to PSI and PSII. Phycobilisomes are composed of many linker proteins and phycobiliproteins, which are proteins with bound chromophores (phycobilins). Excitation energy is transferred from the phycobiliproteins to special chlorophylls comprising the reaction centers of Photosystem II and I, designated respectively, P_{680} and P_{700} (Liu et al., 2005).

PSII is a dimer, composed of an inactivated monomer and an activated monomer. Surprisingly, both monomers have the same subunits and both form a manganese cluster (Loll et al., 2005). PSII is structurally composed of many subunits: CP43, CP47, D1, D2, cytochrome b_{559} alpha and beta subunits, manganese stabilizing protein (MSP), cytochrome c-550 (cyt c-550), 12-kDa protein, PsbQ protein and PsbP protein. In PSII, the MSP, cyt c-550, 12-kDa protein, PsbQ protein and PsbP protein are extrinsic proteins while the rest of the subunits are intrinsic proteins embedded in the thylakoid membrane (Roose et al., 2007a; Roose et al., 2007b; Bricker and Burnap, 2005). PSII also contains protein bound light-absorbing pigments (chlorophyll and carotene), electron carriers (plastoquinones molecules Q_A and Q_B and pheophytin) and inorganic ions (manganese, chloride and calcium).

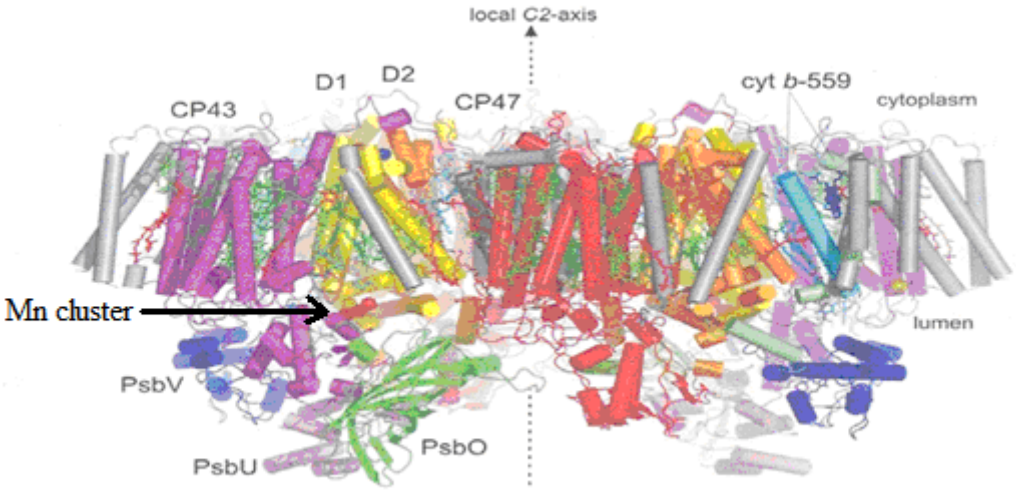

Figure 1. A recent crystal structure of PSII at 3.0 Å resolution. The Mn cluster is represented as the red spheres. (Adapted from Loll et al., 2005)

Energy transferred from the phycobilisomes to the P_{680} reaction center in PSII causes electrons within P_{680} to be excited. P_{680} is composed of two chlorophyll-a molecules, which is the final energy recipient of excitation energy from the phycobilisomes. Excited P_{680}^{*} is oxidized by pheophytin (Pheo), which causes the primary charge separation between $P_{680}^{+\bullet}$ and

$Pheo^{-\bullet}$. Charge recombination between $P_{680}^{+\bullet}$ and $Pheo^{-\bullet}$ can occur, therefore $Pheo^{-\bullet}$ is quickly oxidized by plastoquinone Q_A to form Q_A^- in 250 – 300 picoseconds (ps) (Nelson and Yocum, 2006). $P_{680}^{+\bullet}$ is the strongest biologically occurring oxidizing agent thus able to oxidize water to replenish its electrons. Electrons are again transferred from plastoquinone Q_A^- to plastoquinone Q_B. A nonheme Fe, located along the twofold axis in Figure 1, aids in transferring electrons from plastoquinone Q_A^- to plastoquinone Q_B (Ferreira et al., 2004). Plastoquinone Q_B is capable of accepting two electrons and two protons to form plastoquinol. Plastoquinol is then able to disassociate from photosystem II (Nelson and Yocum, 2006). The functionality and structure of PSII and its constituents will be discussed in greater detail in other sections.

Cyt b_6f is another thylakoid-embedded dimer, which acts to transfer electrons from plastoquinol to plastocyanin and also translocates protons into the lumen in the process. Electrons transferred within Cyt b_6f can follow two pathways: high potential or low potential pathway. Plastoquinol when oxidized releases two electrons to Cyt b_6f and two protons into the lumen. One of these electrons follows the high potential pathway which leads to the reduction of plastocyanin. The second electron follows the low potential pathway which leads to the reduction of one of two internal hemes. When a second plastoquinol is oxidized, both of the internal hemes are reduced, along with another molecule of plastocyanin being reduced. These hemes bound in Cyt b_6f are then finally oxidized by plastoquinone Q_B causing additional protons to be translocated from the stroma into the lumen. This cycle of transporting protons and electrons is referred to as the ‘Q cycle’ (Breyton, 2000; Cramer and Zhang, 2006).

Plastocyanin is a single electron carrier that is reduced by Cyt b_6f and oxidized by PSI (Breyton, 2000). PSI, though it shares similarities with PSII, is a vastly different subunit. PSII replenishes electrons lost to the electron transport chain by oxidizing water whereas PSI oxidizes

plastocyanin. The electron transport chain of PSI varies from the electron transport chain of PSII. PSI includes the following subunits in its electron transport chain: chlorophyll a/a' dimer, chlorophyll a monomer, phylloquinone, and a 4Fe-4S cluster. This reaction center has two semi-symmetrical branches, each capable of allowing electron transport to the first 4Fe-4S cluster. Just like in PSII, the phycobilisomes transfer excitation energy to the PSI reaction center, P_{700}.

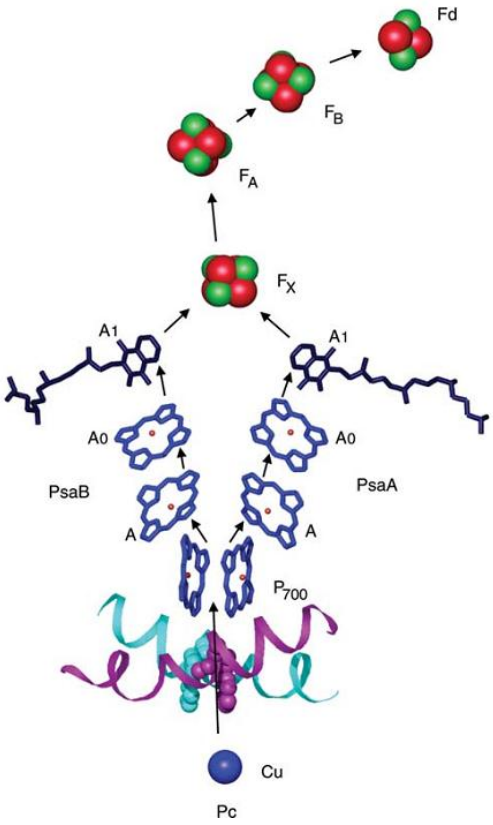

Figure 2. PSI electron transport involving chlorophyll a/a' dimer, chlorophyll a monomer, phylloquinone, and a 4Fe-4S cluster. (Adapted from Nelson and Yocum, 2006)

P_{700} is a chlorophyll-a/a' dimer that forms the first primary charge separation between P_{700}^{+} and A_0^{-}. A_0 is a chlorophyll-a molecule that is part of the reaction center in PSI. Electrons are then transferred to a phylloquinone molecule, A_1. P_{700} to A_1 in the reaction center forms the semi-symmetrical branches; each branch can undergo reduction/oxidation to transfer electrons to F_X. F_X, F_A, and F_B are composed of 4Fe-4S cluster; each cluster acting as electron acceptors in

PSI. F_B is the final electron acceptor associated with PSI and is oxidized by ferredoxin (Fd) (Nelson and Yocum, 2006).

Fd is a 2Fe-2S cluster protein and is reduced by F_B in the stroma. Fd then binds to ferredoxin-NADP(H)-oxidoreductase (FNR). In plants, Fd can only be oxidized when bound to FNR; however in cyanobacteria, Fd can be both oxidized or reduced. Fd binds FNR near the FAD moiety which initiates oxidation of Fd. FNR then reduces a bound molecule of $NADP^+$, causing $NADP^+$ to also be protonated in the stroma (Medina, 2009). Fd can also reduce cyt b_6f or Q_b in a process known as cyclic phosphorylation. Cyclic phosphorylation drives adenosine triphosphate (ATP) synthesis by translocation of protons into the lumen and bypassing photosystem II and the reduction of $NADP^+$.

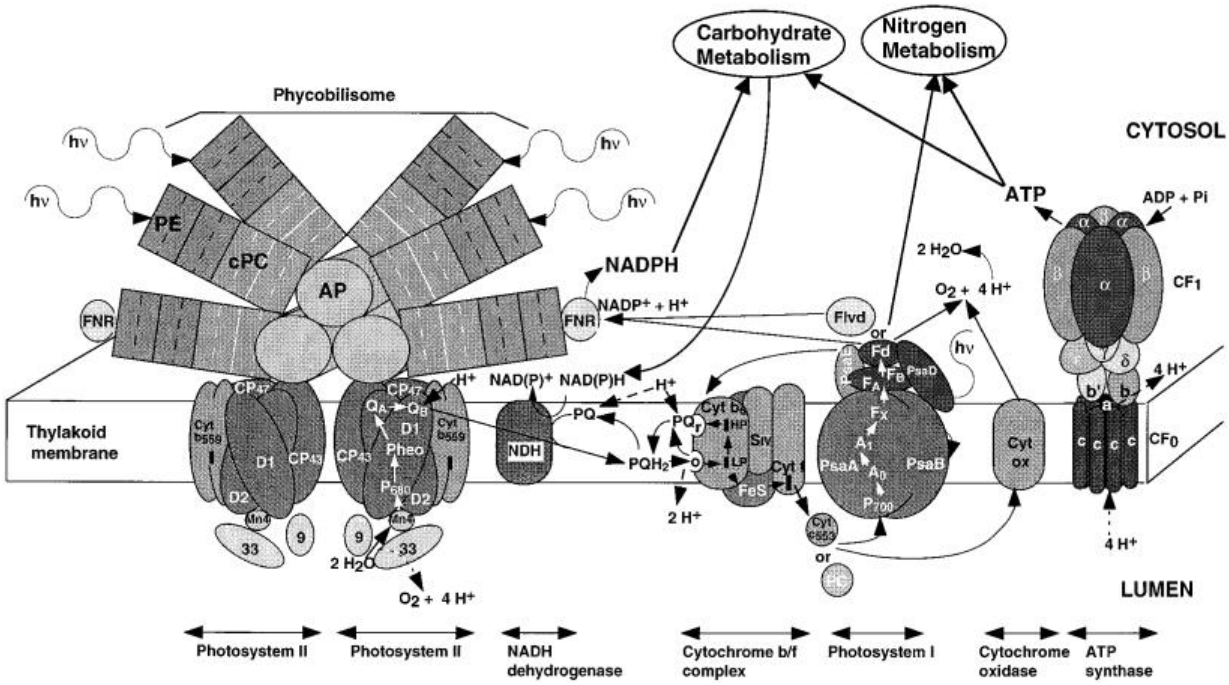

Figure 3. Cyanobacterial thylakoid electron transport. (Adapted from Campbell et al., 1998)

This overall process described above drives protons from the stroma into the lumen. Oxidation of water by PSII releases four protons into the lumen. Also, oxidation of plastoquinol

by Cyt b_6f results in movement of protons into the lumen. Finally, $NADP^+$ is reduced and protonated in the stroma, reducing the proton concentration in the stroma. All of these processes help build a proton electrochemical gradient in the lumen. ATP synthase generates ATP by binding inorganic phosphate and adenosine diphosphate (ADP) by coupling proton transport from the lumen to the stroma (Bienert et al., 2009). This process generates ATP that is used in the Calvin cycle. The Calvin cycle utilizes NADPH and ATP generated by the photosystems for carbon dioxide fixation. The organic molecules synthesized during the Calvin cycle are then further used in other catabolic pathways.

Manganese Cluster

Photosystem II subunits function together to oxidize water but the functions of all the subunits are not well defined. As already stated above, the excited electron in the P_{680} is transported to Cyt b_6f via redox reactions. $P_{680}^{+\bullet}$, the strongest oxidizing agent known in nature, replenishes the lost electron from a near-by tyrosine (TyrZ or Y_z) (Debus et al., 1988). TyrZ is amino acid 161 of subunit D1. TyrZ when oxidized forms a neutral radical because electron transfer is also followed by a proton transfer from a nearby histidine; proton and electron transfer provides a charge balance (Vrettos and Brudvig, 2002). TyrZ is then reduced by a Mn_4CaCl_x cluster, often referred to as the manganese cluster. Four consecutive oxidations of the manganese cluster results in the oxidation of two water molecules to form four protons, one diatomic oxygen and four electrons (Joliot, 1968; Kok et al., 1970). Oxidation of water to replenish electrons in PSII is so highly innovative because of the nearly endless supply of water that can be used as a fuel source.

Dark-adapted algal suspensions exposed to single turnovers of actinic light release diatomic oxygen in highest amounts initially on the third flash (Joliot, 1968; Kok et al., 1970).

After the third flash, every fourth flash results in peak release of diatomic oxygen. Based on those experimental results, the S-state cycle was developed. The S-states infers the oxidation states of the manganese cluster. The S_0 state is the most reduced state, while the S_4 state is the most oxidized state. The S_1 state is dark stable and can be thought of as the ground state. Failure to advance S-states results in higher S-states being reduced back to the S_1 state (Kok et al., 1970). Diatomic oxygen is released when incoming photons advance the cycle forward from the S_3 state to the S_0 state. Not until recently has the elusive S_4 state been observed (Haumann et al., 2005). The failure to observe the S_4 state until recently has been due to the fact that it is a transient state. The S_4 state forms before the formation and release of diatomic oxygen, and involves a deprotonation process.

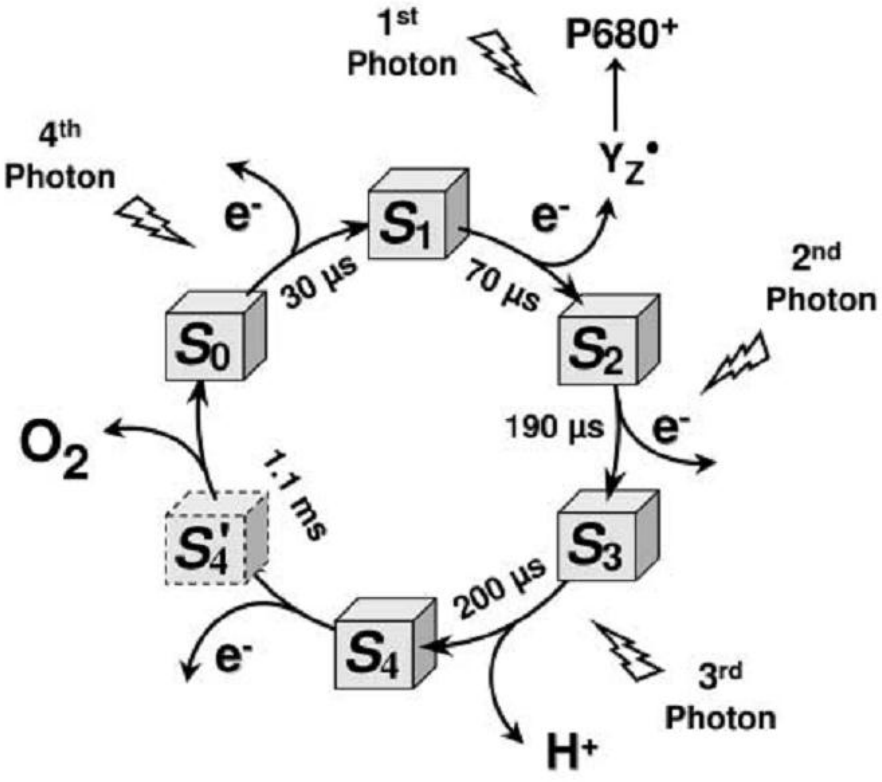

Figure 4. S-state mechanism of the OEC which oxidizes two water molecules to produce a diatomic oxygen in a stepwise manner. (Adapted from Haumann et al., 2005)

The manganese cluster is composed of four atoms of manganese, a single atom of calcium and also a chloride ion. Until recently, the position of chloride in the cluster was unknown. Chloride in the oxygen evolving complex is 6.5 ångströms (Å) away from the manganese cluster (Guskov et al., 2009). Chloride's position away from the manganese cluster also agrees with previous findings that the chloride ion should be at least 5 Å away from the cluster (Haumann et al., 2006). The manganese cluster's exact structure is the topic of much debate because techniques such as x-ray crystallography reduce the manganese cluster, breaking bonds, causing the manganese cluster's ligand field to be modified (Yano et al., 2005). Other techniques, such as x-ray absorption spectroscopy, which utilize lower amounts of radiation, can provide valid information about the manganese cluster.

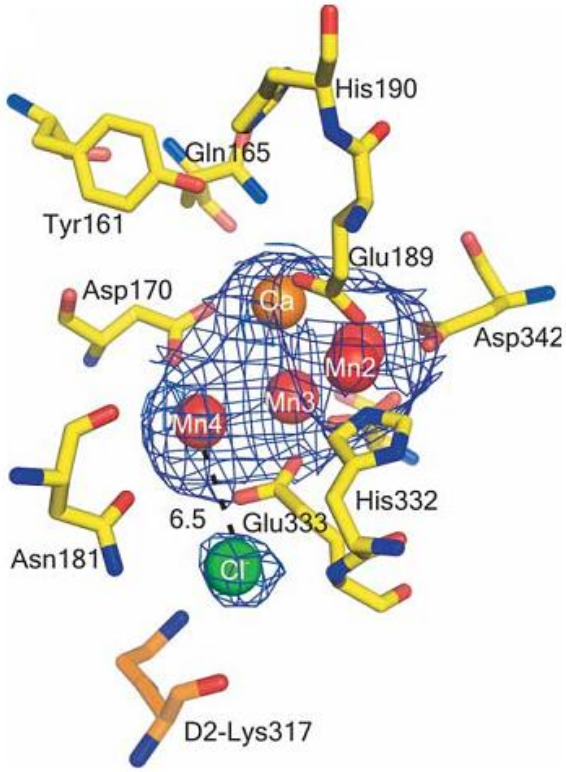

Figure 5. The manganese cluster of PSII and the Cl^- binding site. (Adapted from Guskov et al., 2009)

Both calcium and chloride are required for $S_2 \rightarrow S_3$ and $S_3 \rightarrow S_4 \rightarrow S_0$ transitions (Miqyass et al., 2007; Popelkova and Yocum, 2007). Although both these ions are needed for S-state advancement, the roles are still undefined. Chloride is thought to function as a charge neutralizer for the manganese cluster or to maintain the structure of a proton exit channel from the oxygen evolving complex to the lumen (Guskov et al., 2009). The role of chloride in the oxygen evolving complex has been elusive but it's proposed functions are: ligation to the manganese cluster, regulating the redox potential of the manganese cluster, maintaining a hydrogen bond network around the manganese cluster, and maintaining a proton exit channel (Kawakami et al., 2009). Calcium, on the other hand, might play a structural role. However, calcium is thought to function as a Lewis acid, adding more complexity to the ligand field (Lee et al., 2007).

Currently, there is a debate as to whether one or two chloride ions bind to the oxygen evolving complex. Recent crystal structure of PSII at 2.9 Å resolution revealed one chloride ion 6.5 Å away from the manganese cluster (Guskov et al., 2009). Also, only one radioactive $^{36}Cl^-$ was retained in isolated PSII (Lindberg and Andreasson, 1996). Based on bromide-substituted crystal structure, Kawasami and coworkers (2009) found two bromide binding sites in PSII. Since bromide ions can be used as a substitute for chloride ions, this suggests two binding sites for chloride ions.

Divalent calcium was replaced with other divalent and trivalent cations such as Cd^{+2}, Sr^{+2} and Dy^{+3} and the effect of these replacements were investigated. Dy^{+3} and Cd^{+2} allow for $S_1 \rightarrow S_2$ advancement but Sr^{+2} is the only substitution in place of calcium that allows for diatomic oxygen release. Based on the studies it was determined that calcium plays a structural role in the early S-states but a functional role for the advancement of S-states after the S_2 state (Lee et al.,

2007). It should be noted that both divalent strontium and calcium have similar Lewis acidities though strontium has a larger radii; aqua ion bound to calcium has a pK_a of 12.80 while aqua ions bound to strontium has a pK_a of 13.18 (Brudvig, 2008).

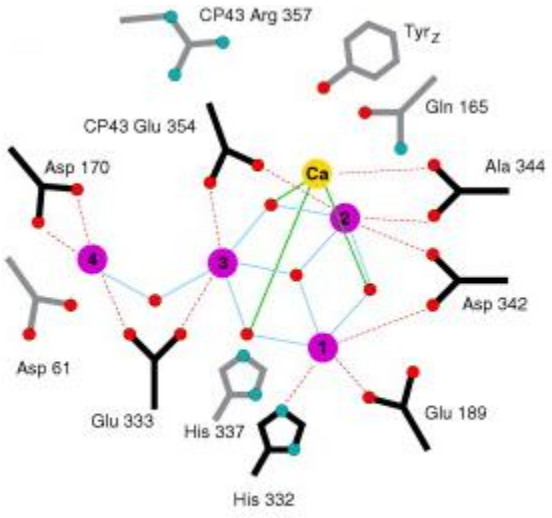

Figure 6. A refinement of the water splitting site using the electron density maps of Ferreira et al., (2004) and Yano et al., (2006) keeping the $Mn_3Ca^{2+}O_4$-cubane but with Mn4 linked to it via a single 3.3 Å mono-μ-oxo bridge. (Adapted from Barber and Murray, 2008)

The mechanism of water oxidation into diatomic oxygen formation is fundamental to understand photosynthesis. Recent experimental data, as discussed above, suggests that calcium functions as Lewis acid and has a crucial role as a water (or hydroxyl) binding site. Water, bound to calcium, undergoes a nucleophilic attack of a oxygen atom bound to a manganese atom, leading to the formation of diatomic oxygen (Brudvig, 2008) . This process occurs during the $S_3 \rightarrow S_4 \rightarrow S_0$ transition but fails to explain why divalent calcium is required for $S_2 \rightarrow S_3$ transitions (Miqyass et al., 2007) . Therefore, replacement of calcium with other metals would require a metal with the same Lewis acidity such as strontium. When strontium replaced calcium in PSII, bound water was accelerated 3-5 times within the OEC, indicating that calcium binds water

molecules and strontium fails to bind water as efficiently as calcium (Hendry and Wydrzynski, 2003). Water bound at terminal atoms (terminal aqua) exchange at a faster rate than water bound to μ-O ligands between the metal atoms (Tagore et al., 2006; Tagore et al., 2007). This exchange rate is crucial because water must be replaced within the proper time scale for efficient OEC turnover. It is likely that the terminal metal for water binding is calcium.

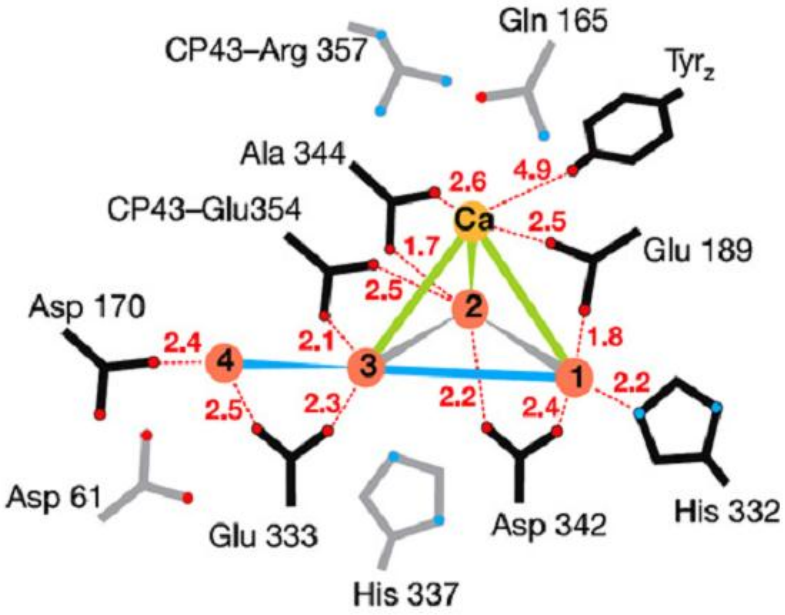

Figure 7. Mn_4Ca^{2+} cluster adapted from Loll et al., (2005) with distances between the ligands and the cluster shown in red; blue lines represents a distance of 3.3 Å, green lines represents a distance of 3.4 Å, and grey lines represents a distance of 2.7 Å. (Adapted from Barber and Murray, 2008)

The manganese cluster is isolated from the aqueous environment by both the intrinsic and extrinsic proteins. Three of the manganese atoms are bonded together by di-μ-oxo-bridges, while a fourth manganese atom is linked to the cluster through a mono-μ-oxo-bridge. Recent models of the manganese cluster places calcium coordinated to the cluster (Ferreira et al., 2004; Guskov et al., 2009; Loll et al., 2005) and ligands to the cluster based on these structures have been identified. Three of the manganese atoms and divalent calcium form a cubane structure

with a fourth manganese atom dangling away from the cluster (Ferreira et al., 2004). The distance between the manganese atoms were measured to be ~2.7 Å while the distance between manganese and calcium was ~3.4 Å. The fourth "dangling" manganese atom's distance from the cubane was ~3.3 Å, typical of a mono-μ-oxo bridge.

The cubane manganese cluster proposed by Ferreira et al., (2004) was the first complete PSII structure and also allowed for the modeling of ligands that bind the manganese cluster. However, the model lacks depth due the resolution of the x-ray structure at 3.5 Å. The model initially provided no ligands to the calcium metal, but later was modified taking into account other x-ray spectroscopy data, as shown in Figure 6. Loll et al., (2005) published a different arrangement of the manganese cluster, Figure 7, in which the manganese cluster's geometry resembled a trigonal pyramidal structure rather than a cubane structure. However, both structures agreed on the positions of the subunits, calcium and also the fourth "dangling" manganese atom. The fourth "dangling" manganese atom plays no role in the oxidation based on FTIR difference spectroscopy of mutant D1-D170H; the same amino acid shown in Figures 6 and 7 as a ligand to the fourth manganese (Debus et al., 2005). The positions and the ligands that bind the other three manganese atoms differ in the two models. However, both models identify an alanine amino acid as a bidentate, which is a C-terminal residue of the D1 subunit.

Photosystem II Subunits

PSII is structurally composed of many subunits: CP43, CP47, D1, D2, cytochrome b_{559} alpha and beta subunits, MSP, cyt c-550, 12-kDa protein, PsbQ protein and PsbP protein. The subunits that comprise PSII and their functions are listed in Table 1. As seen in Figures 5-7, the manganese cluster is coordinated by PSII subunits. Intrinsic PSII proteins are evolutionarily conserved from cyanobacteria to plants. Though only intrinsic proteins are necessary for

diatomic oxygen evolution, extrinsic proteins are needed for maximum rates of diatomic oxygen release. MSP is the only conversed extrinsic subunit in all photosynthetic organisms (Roose et al., 2007b; Bricker and Burnap, 2005).

D1 and D2 subunits are integral components of PSII. They bind/coordinate important cofactors such as: tyrZ, tyrD, manganese atoms, Pheo, Q_A, and Q_B. As shown in Figures 5-7, D1 also provides ligands to the manganese cluster. Mutagenesis of these residues added experimental proof that they provide the ligand field for the manganese cluster (Debus, 2008). The D1 subunit is regularly damaged causing photoinactivation of PSII. When PSII is exposed to high intense light, the rate of damage exceeds the rate of repair, causing photoinactivation (Nishiyama et al., 2005). The repair process involves the degradation and removal of the D1 subunit, then the synthesis of the precursor to the D1 protein which is used to assemble the new PSII complex, and finally processing the precursor D1 subunit to produce a mature D1 subunit (Mohanty et al., 2007).

Cyt b559 alpha and beta subunits coordinate a heme group but the function of the subunits is still unknown (Pakrasi et al., 1989). Cyt b559 alpha and beta are thought to have a structural role in PSII (Nelson and Yocum, 2006). Other possible functions include a role in cyclic photophosphorylation and protection of PSII from photoinactivation.

CP43 and CP47 are chlorophyll binding proteins. According to the latest x-ray crystal structure, CP43 binds fourteen chlorophylls and CP47 binds sixteen chlorophylls (Ferreira et al., 2004; Loll et al., 2005). Histidine residues coordinate chlorophyll molecules (Manna and Vermaas, 1997). Chlorophylls bound to CP43 and CP47 can absorb light energy and transfer the energy to the reaction center. Deletion of *psb*B or *psb*C genes, results in loss of photoautotrophic growth and loss of core complex assembly in PSII (Clarke and Eaton-Rye, 2000).

Table 1. Intrinsic and extrinsic subunits of Photosystem II Required for Optimal Function

Gene	Gene Product	Association with the Thylakoid Membrane	Proposed Function(s)
psbA	D1 protein	Intrinsic	PSII reaction center component; contains Y_Z; together with the D2 protein, binds P680; provides majority of ligands to OEC
psbB	CP47 protein	Intrinsic	Chlorophyll-a antennae; lumenal interactions with other PSII components
psbC	CP43 protein	Intrinsic	Chlorophyll-a antennae; lumenal interactions with other PSII components including OEC
psbD	D2 protein	Intrinsic	PSII reaction center component; together with the D1 protein, binds P680
psbE	Cytochrome $b_{559}\alpha$	Intrinsic	Core antenna component of the PSII reaction center; involved in water oxidation; together with the β subunit, stabilizes the PSII reaction center and may help protect PSII from photochemical damage
psbF	Cytochrome $b_{559}\beta$	Intrinsic	A component of the PSII reaction center; together with the α subunit, stabilizes the PSII reaction center and may help protect PSII from photochemical damage
psbO	33-kDa protein (Manganese Stabilizing Protein)	Extrinsic (Lumen)	Stabilizes manganese cluster; lowers calcium and chloride requirements
psbP	PsbP Protein	Extrinsic (Lumen)	Only found in Cyanobacteria; unknown function
psbQ	PsbQ protein	Extrinsic (Lumen)	Only found in Cyanobacteria; stabilizes OEC for optimal PS II function
psbU	12-kDa protein	Extrinsic (Lumen)	Links 33-kDa protein and cytochrome c_{550}; provides a stable architecture for the OEC to operate optimally
psbV	Cytochrome c_{550}	Extrinsic (Lumen)	Helps stabilize the OEC and PSII; shields the OEC

Structurally, CP43 and CP47 are similar, containing six transmembrane alpha helices and also five hydrophilic loops. Three of these loops extend into the lumen, labeled loops A, C, and

E. The largest of these loops in CP43 and CP47 is loop E and both have been extensively mutated. Loop E in CP47 does not provide any direct ligands to the manganese cluster. However, loop E in CP43 provides ligands both to the manganese cluster and to the extrinsic proteins (Bricker et al., 2002; Han et al., 1994). CP43-Glu354 appears to coordinate two manganese ions as a bridging bidentate ligand in the S_1 state and a single manganese ion in the higher S-states. Based on Fourier transform infrared difference data indicating an OH stretching vibration of an active water molecule bound to a manganese ion during the S_2/S_1 states, it is believed that the manganese ion coordinated in the higher S-states by CP43-Glu354 also binds a water molecule. Mutation of Glu354 produces mutants that have a lower oxygen evolving activity compared to the wild-type and also a slower growth rate (Rosenburg, et al., 1999; Shimada et al., 2009). CP43-Arg357 might coordinate the manganese cluster through bicarbonate or be involved in proton-coupled electron transfer in higher S-states. It is also possible that CP43-Arg357 is involved in binding chloride (Hwang et al., 2007). Mutation of Arg357 produces mutants incapable of evolving oxygen (Knoepfle et al., 1999).

Mutation of arginine at position 305 in CP43 to a serine residue (R305S), produced a mutant with severely reduced growth and oxygen evolving activity under chloride limiting conditions (Knoepfle et al., 1999; Young et al., 2002). However, when grown under normal conditions, the R305S mutant showed no extreme phenotype. After isolation of PSII particles and chemiluminescent staining, it was determined that this specific mutation resulted in loss of binding of an extrinsic PSII protein, cyt c-550 (Bricker et al., 2002).

The arginine residue at position 305 was further investigated by mutating the arginine residue to either a lysine or an aspartic acid (Burch, 2003). Both the mutations resulted in reduced growth and oxygen evolving activity under chloride limiting conditions; however some

mutations had a more pronounced effect than others. The mutations can be ranked from having the most effect on photoautotrophic growth and oxygen evolving activity to the least effect in chloride limiting media: R305D > R305S > R305K. These mutants were more susceptible to photoinactivation than the control, indicating that the mutations decreased the stability of the PSII complex. It appears that a positive charge is required at this site for function since only the R305K mutant strain was able to grow photoautotrophically in chloride-limiting media and evolve oxygen at control rates (Burch, 2003).

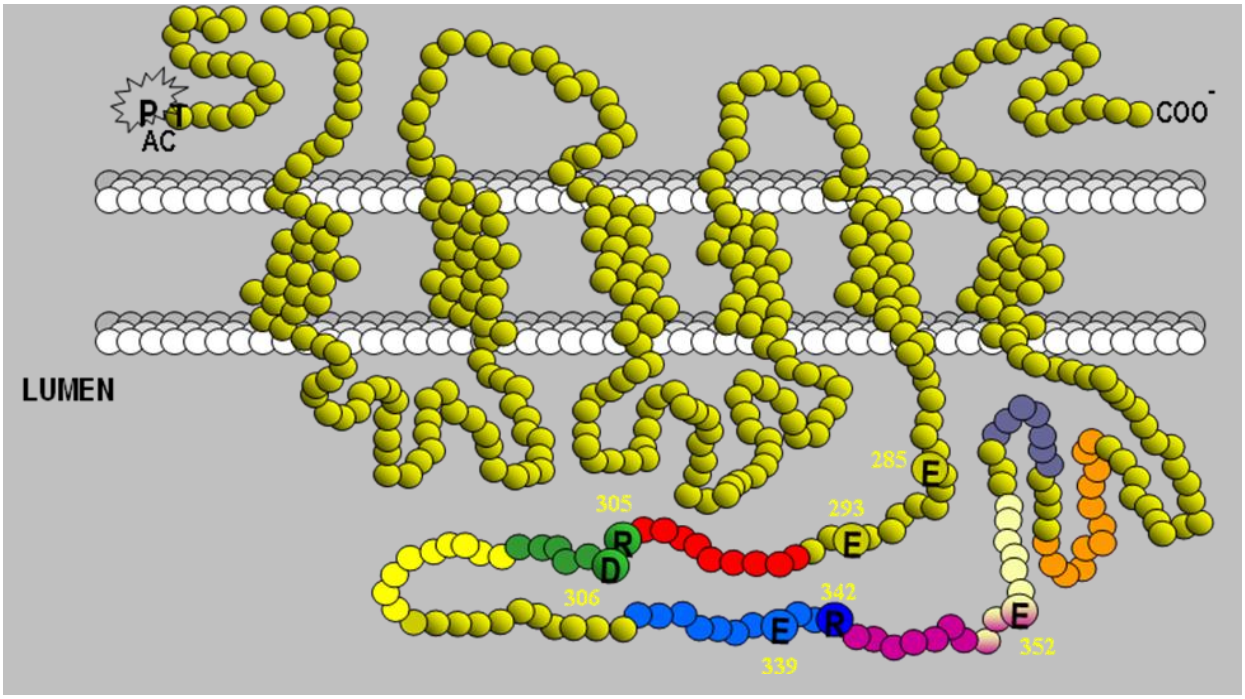

Figure 8. Model of the CP43 protein from *Synechocystis*. The Large Extrinsic Loop E (LEL) occurs between the 5th and 6th membrane spanning domains. Deletion mutations in the LEL produced by Vermaas, which exhibited a PSII-minus phenotype are indicated by colors. Site-directed mutations with impaired PSII function produced by Putnam-Evans are indicated by the one-letter amino acid abbreviation.

Cyt c-550 is a small heme-coordinated protein (15 kDa) with dominantly alpha helical characteristics with the exception of a short two-stranded beta sheet near the N-terminus (Kerfeld et al., 2003). Hemes contain an iron bound porphyrin macrocycle, in which the iron is coordinated by nitrogens of the marcocycle and also two axial ligands donated by the protein. C-

type hemes are attached to the protein through two cysteine residues via thioether linkages. Cyt c-550 heme binding sequence motif is Cys-X-X-Cys-His; this binding sequence motif is conserved in all c-type cytochromes (Bricker and Burnap, 2005). This protein is unusual, because it's counterpart in higher organisms, the PsbP protein, does not coordinate a heme group. Cyt c-550 also has an unusually low redox potential (Enami et al., 2008). The redox potential of cyt c-550 in solution is -240mV, but when bound to PSII the redox potential increases to -80mV (Vrettos et al., 2001). The low redox potential in solution is due to the heme exposure to the aqueous environment, which is shielded when bound to PSII. Exposure of the heme is largely due to the propionic group D, but more specifically D-propionate oxygen atoms which are not buried within cyt c-550 (Ishikita and Knapp, 2005; Kerfeld et al., 2003). Also, the heme group is coordinated axially by bishistidine; histidine tends to donate more electrons than other amino acids such as cystine and methionine (Mao et al., 2003). Therefore, it is not surprising that hemes coordinated by histidines tend to have lower redox potentials.

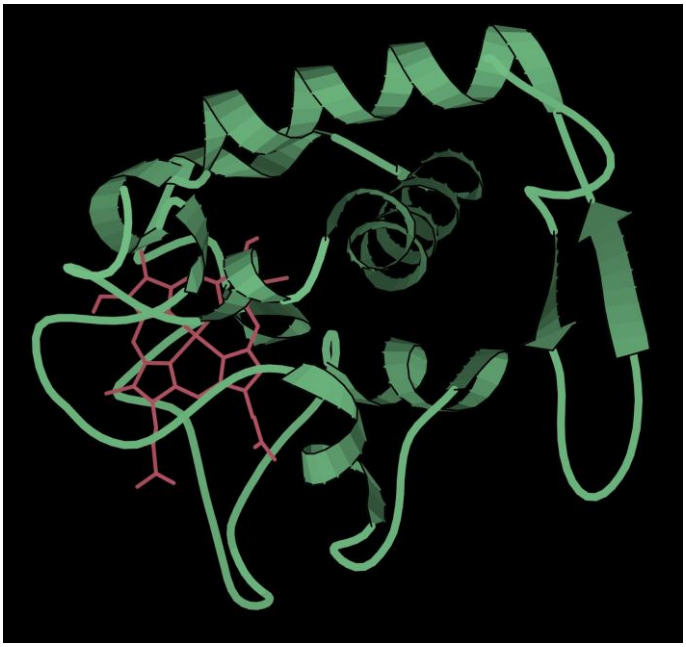

Figure 9. Ribbon structure of Cytochrome c-550 adapted from the crystal structure of PSII at 3.0 Å resolution. (Adapted from Loll et al., 2005)

When soluble, cyt c-550 is present as a dimer; the dimer interface consists of D-propionate oxygen atoms and an asparagine residue on cyt c-550. As noted before, the propionic group D is exposed to the environment when not bound to PSII and probably causes the lower redox potential when unbound (Kerfeld et al., 2003). Propionic group D is near a β-turn around asparagine at position forty nine. When cyt c-550 is isolated in its monomeric and dimeric form, the carbonyl groups on the backbone of the β-turn are oriented towards the heme, stabilizing the oxidized state. Cyt c-550 bound to PSII repositions the carbonyl groups, and CP43-Arg305 might enforce the reorientation of the backbone carbonyl groups (Ishikita and Knapp, 2005).

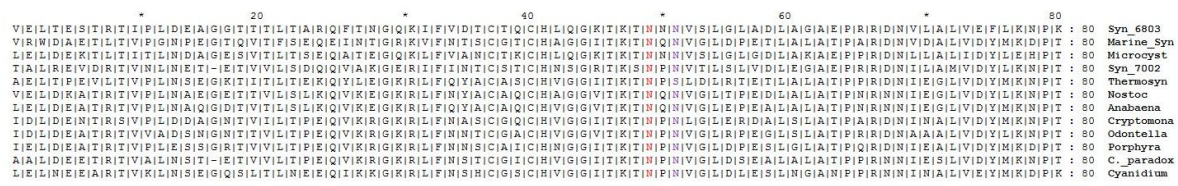

Figure 10. PsbV Alignment of the amino acid sequences (residues one to eighty shown) of cyt c-550 (PsbV) from twelve different organisms with amino acids highlighted at position forty nine and fifty one. (Adapted from Bricker and Burnap, 2005)

Deletion of *psb*V gene results in the loss of photoautotrophic growth in media lacking chloride and/or calcium (Andrews et al., 2005; Shen et al., 1995). In complete media, the strain grows photoautotrophically. Not surprisingly, when the PsbP protein in higher plants is removed from PSII, the same dependence on calcium and chloride is observed. Deletion of both *psb*O and *psb*U genes yields the same results as deletion of *psb*V (Enami et al., 2008; Roose et al., 2007b; Bricker and Burnap, 2005). The most pronounced effect is the deletion of *psb*O, which results in lower accumulation of other extrinsic proteins. It has been widely speculated that release of the extrinsic proteins from the oxygen evolving complex hinders the ability to retain calcium and chloride ions. The extrinsic proteins stabilize the ion environment for oxygen evolution but the functionality of the heme coordinated by cyt c-550 is still largely unknown. Cyt c-550's heme is

positioned 25.7 Å from the manganese cluster (Wydrzynski, 2008). It has been speculated that cyt c-550 might play a role in cyclic phosphorylation. Cyt c-550 has been shown to undergo reduction by ferredoxin (Kang et al., 1994).

A distal axial heme ligand in cyt c-550, His92, was mutated to a methionine residue (H92M). This mutation did cause the accumulation of PSII complex to decrease but the interaction between cyt c-550 and PSII was not affected. Also, the mutant does function as the sixth heme ligand. The H92M mutant has reduced photoautotrophic growth in calcium lacking media but not in chloride lacking media (Li et al., 2004).

In another study, specific amino acids on cyt c-550 were mutated to disrupt the redox potential; mutagenesis of amino acids that impact the redox potential of cyt c-550 did not alter the function of the subunit (Andrews et al., 2005). All the mutants' heme groups were capable of undergoing reduction/oxidation. Therefore, the functionality of the heme group is still ill-defined.

CHAPTER 2: RESEARCH PROBLEM

Photosytem II is a multi-subunit complex, bound within the thylakoid membrane, which is an integral component of the photosynthetic apparatus of higher plants, cyanobacteria and green algae. Photosystem II catalyzes the oxidation of water and reduction of plastoquinone. Oxidation of water is accomplished by a tetramanganese-Ca-Cl_x cluster bound to the integral proteins D1, D2, and CP43of photosystem II. This complex is more commonly referred to as the oxygen evolving complex. The oxygen evolving complex is capped by extrinsic proteins (manganese stabilizing protein, cytochrome c-550 (cyt c-550), and 12-kDa protein in cyanobacteria), which appear to concentrate chloride and calcium at the active site.

A mutation at an arginine residue at position 305 to serine, on protein CP43, produced a cyanobacterial mutant that failed to grow photoautotrophically in media lacking chloride ions (Knoepfle et al., 1999; Young et al., 2002). It was shown that this specific mutation resulted in loss of binding of an extrinsic protein, cyt c-550 (Bricker et al., 2002). Deletion of the *psb*V gene, which encodes for the cyt c-550 protein, produced a mutant with a similar phenotype (Shen et al., 1998). However, in chemical crosslinking experiments, CP43 and cyt c-550 were not identified as having any crosslinked products (Han et al., 1994). X-ray crystallography of PSII (PDB: 2AXT) does in fact show a close proximity between cyt c-550 and CP43 (Loll et al., 2005). Based on this crystal structure, two residues on cyt c-550 were identified that might interact with CP43 and are in close proximity with the arginine residue at position 305. These residues on cyt c-550 are both highly conserved asparagines, located at positions forty nine and fifty one. In this work, the asparagine residue at position fifty one on cyt c-550 was mutated to either an alanine or aspartic acid residue. The N51 mutations were transformed into wildtype *Synechocystis*, a cyanobacterial model organism that has been widely used to study PSII. The

N51 mutants were characterized by photoautotrophic growth in complete and chloride-limiting media, oxygen evolution assays, variable florescence yield measurements and photoinactivation assays.

CHAPTER 3: MATERIALS AND METHODS

Isolation of Genomic DNA from *Synechocystis* 6803

A small amount of cyanobacterial cells was scraped off stock plates and resuspended in 500 µL of BG11 media. The cells were vortexed and then centrifuged at 6,000 revolutions per minute (rpm) in an Eppendorf microcentrifuge for one minute. The supernatant was removed and the pellet was resuspended in 400 µL of Buffer A (5 mM Tris-HCl pH 8.0, 50 mM NaCl, 5 mM ethylenediaminetetraacetic acid (EDTA)). 100 µL of lysozyme (50mg/mL) was added to the solution and then incubated at 37°C for fifteen minutes. After the incubation, the following reagents were added in the order listed: 20 µL of 500 mM EDTA, 50 µL of proteinase K (10mg/mL) in 50% glycerol, and 55 µL of 10% sarkosyl. Then the samples were incubated at 55°C for fifteen minutes and allowed to cool for five minutes. 600 µL of TE-saturated phenol was added to the samples and incubated at room temperature for ten minutes. The samples were centrifuged at 14,000 rpm for three minutes. After centrifugation, the aqueous layer was transferred to a new microcentrifuge tube and the following regents were added: 100 µL of 5 M NaCl, 100 µL of 10% cetyl trimethylammonium bromide (CTAB), and 600 µL of chloroform. The microcentrifuge tubes were placed on a rotary shaker at 200 rpm for fifteen minutes. The samples were centrifuged at 10,000 rpm for three minutes and the aqueous phase was once again transferred to a new microcentrifuge tube. An equal volume of cold 100% isopropanol was added and the microcentrifuge tubes were inverted slowly several times and incubated at room temperature for twenty minutes. Following the incubation, the samples were centrifuged at 10,000 rpm for ten minutes at 4°C. The supernatant was then removed and 1 mL of cold 70% ethanol was added. The samples were then again centrifuged at 10,000 rpm for ten minutes at 4.0°C. The supernatant was removed and the samples were dried in a Jouan RC1010 rotary

speed vacuum. The pellet was resuspended in 100 µL of filtered sterilized water. The sample was then analyzed by agarose gel electrophoresis.

Amplification of *psb*V

Table 2. Primers for Amplification of *psb*V

Name of Primer	Sequence
*psb*V 5'	TTG CCC TCG AGG ACG CTA AA
*psb*V 3'	AAA ACC ATC TCC CAA TGC TG

Gene *psb*V encoding cytochrome c-550 was amplified by polymerase chain reaction (PCR). A 50 µL reaction tube was prepared consisting of 1X PCR Buffer, 0.2 mM dNTP, 1.5 mM MgCl2, 0.5 µM *psb*V 5', 0.5 µM *psb*V 3', 4 µL of genomic DNA (genomic DNA was isolated from *Synechocystis* 6803 strain *psb*C) and 2.5 units of recombinant Taq DNA polymerase. The samples were placed in a thermal cycler and the following protocol applied: Step one, 94.0°C for 2.5 minutes; step two, 94.0°C for forty-five seconds; step three, 50.0°C for 45 seconds; step four, 72.0°C for one minute; step five, go to steps two to four 25 times; step six, 72.0°C for fifteen minutes; step 7, 4.0°C hold. The PCR amplified region was 1373 base pairs and the length of the product was verified by gel electrophoresis.

Creation of Plasmid pAM1

Ligation reactions were prepared consisting of 1X Rapid Ligation Buffer, 50 ng of pGEM®-T vector, 70 ng of PCR amplified *psb*V, and three units of T4 DNA ligase to equal a total volume of 10 µL. The reaction was left at room temperature for one hour. Then 2.0 µL of the ligation reaction was used to transform the plasmid into JM109 Competent Cells (see below). 100 µL of the JM109 Competent Cells were plated on a LB plate containing ampicillin and incubated overnight at 37.0°C. Individual colonies were then selected and isolated. Screening of the plasmids included digestion of the plasmid with restriction enzymes HindIII, XbaI, and XhoI while the length of the restriction digests products were verified by gel electrophoresis.

Creation of Plasmid pAM3

Digestion of plasmid pBSL14 (provided by Dr. Paul Hager, East Carolina University) with restriction enzyme XbaI yielded a kanamycin resistance gene cassette (Alexeyev, 1995). This gene was isolated and cleaned by agarose gel extraction. Plasmid pAM1 cleaved by restriction enzyme XbaI was also isolated and cleaned by agarose gel extraction. The kanamycin resistance gene cassette and cleaved pAM1 were ligated and then transformed into JM109 Competent Cells (see below). 100 µL of the JM109 Competent Cells were plated on a LB plate containing kanamycin. Individual colonies were then selected and isolated. Screening of the plasmids included digestion of the plasmid with restriction enzymes HindIII, XbaI, and XhoI while the length of the restriction digests products were verified by gel electrophoresis. The kanamycin resistance gene cassette is only three base pairs downstream of the *psb*V gene. The XbaI recognition site also forms the stop codon for the *psb*V gene.

Transformation into E. Coli strain JM109

100 µL of JM109 Competent Cells were transferred into pre-chilled microcentrifuge tubes. Added 7.5 ng of plasmid DNA to the 100 µL of JM109 Competent Cells and flicked the tube several times. The microcentrifuge tubes were immediately placed on ice for thirty minutes. After the incubation, the JM109 Competent Cells were heat-shocked for fifty seconds in a 42.0°C water bath. The microcentrifuge tubes were placed on ice for two minutes. Following the incubation, 900 µL of room temperature SOC medium was added to each reaction and incubated for sixty minutes at 37.0°C on a rotary shaker at 225 rpm. 100 µL of the JM109 Competent Cells were plated on a LB plate containing the appropriate antibiotics. The plates were placed in an incubator at 37.0°C for approximately twelve hours. Individual colonies were then selected and isolated.

Plasmid Purification

Plasmids were purified using a GenElute^{TM} Plasmid Miniprep Kit from Sigma-Aldrich. 1.5 ml of an overnight recombinant E. coli culture was centrifuged at 12,000 rpm in an Eppendorf microcentrifuge to form a pellet and then the supernatant was discarded. 200 µl of the Resuspenion Solution was added and pipetted back and forth to suspend the pellet. 200 µl of the Lysis Solution was added and the pellet was resuspended by mixing the contents by gentle inversion (6–8 times) until the mixture became clear and viscous. Cell debris was precipitated by adding 350 µl of the Neutralization Solution and then inverting the tube 4–6 times. The solution was then centrifuged at 12,000 rpm for ten minutes.

A GenElute Miniprep Binding Column was inserted into a microcentrifuge tube and 500 µl of the Column Preparation Solution was added to each miniprep column and centrifuged at 12,000 rpm one minute and then the flow-through liquid was discarded. The cleared lysate was transferred to the column and centrifuged at 12,000 rpm for one minute and the flow-through liquid was discarded. 750 µl of the diluted Wash Solution was added to the column and the column was centrifuged at 12,000 rpm for one minute. The flow-through liquid was discarded and centrifuged again at 12,000 rpm for one minute to remove excess ethanol. The column was transferred to a fresh collection tube and 100 µl of filter-sterilized water was added to the column. The column was centrifuged at 12,000 rpm for one minute to elude the plasmid DNA.

Site-Directed Mutagenesis

Table 3. Mutagenic Primers

Name	Sequence
CytC550-1	TAA ACT AAC GTT ATT GTC AGT TTT GGT TTT AC
CytC550-2	TAA ACT AAC GTT ATT GGC AGT TTT GGT TTT AC
CytC550-3	CCA AGC CTA AAC TAA CGT CAT TAT TAG TTT TGG TTT TAC

CytC550-4	CCA AGC CTA AAC TAA CGG CAT TAT TAG TTT TGG TTT TAC
CytC550-1'	GTA AAA CCA AAA CTG ACA ATA ACG TTA GTT TA
CytC550-2'	GTA AAA CCA AAA CTG CCA ATA ACG TTA GTT TA
CytC550-3'	GTA AAA CCA AAA CTA ATA ATG ACG TTA GTT TAG GCT TGG
CytC550-4'	GTA AAA CCA AAA CTA ATA ATG CCG TTA GTT TAG GCT TGG

Site-directed mutagenesis was preformed using a procedure known as overlap extension PCR. The procedure requires the use of four primers, including two primers that contain the mutation to be incorporated. Each pair of primers is used to amplify the upstream and downstream sequences from the site of mutation. The products from the upstream and downstream sequences in conjunction with primers used in the ampilication of *psb*V create the full length mutant sequence; this sequence was then ligated into plasmid pGEM®-T. The plasmids were purified and screened to ensure that the orientation of the inserted sequences were correct.

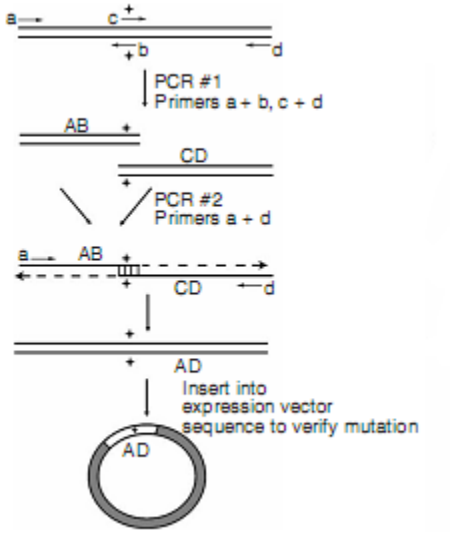

Figure 11. Overview of Overlap Extension PCR (Adapted from Heckman and Pease, 2007)

Transformation into *Synechocystis* 6803

Cultures of wildtype *Synechocystis* were grown at 28ºC with 30 µmole photons m^{-2} s^{-1}, until they reached the mid-exponential phase of growth (Kufryk et al., 2002). The cells were harvested by centrifugation at 3000 rpm for five minutes. The pellet was resuspended in 1 mL of BG11 media. To the concentrated cell mixture, 1 µg of the appropriate mutagenized plasmid (either N51A or N51D) was added. The cells were incubated at the same light intensity as before for five hours. After the incubation period, the cells were plated on plates that contain no antibiotics and allowed to grow for two days. After the two day period, the plates were underlayed with kanamycin (10 µg/mL). Colonies that arose on the plates were selected and sorted out three separate times to allow homozygous transformations of the octoploid genome. Finally, an individual colony was selected and grown in a 100-mL BG11 culture. During the exponential phase of growth, the cells were concentrated and then frozen. Genomic DNA was extracted from each sample and submitted for verification of the intended mutation by DNA sequencing.

DNA Sequencing

Gene *psb*V encoding cytochrome c-550 was amplified by polymerase chain reaction (PCR) from genomic DNA by primers *psb*V5' and *psb*V3'. A 50 µL reaction tube was prepared consisting of 1X PCR Buffer, 0.4 mM dNTP, 1.5 mM MgCl2, 0.5 µM *psb*V 5', 0.5 µM *psb*V 3', 4 µL of genomic DNA and 2.5 units of recombinant Taq DNA polymerase. The samples were placed in a thermal cycler and subjected to the following protocol: Step one, 94.0°C for 1.5 minutes; step two, 94.0°C for forty-five seconds; step three, 50.0°C for 45 seconds; step four, 72.0°C for one minute 45 seconds; step five, go to steps two to four 27 times; step six, 72.0°C for thirty minutes; step 7, 4.0°C hold. The PCR amplified product was cleaned using Sephadex G-

50. The clean PCR products were then sequenced by the genomics lab using a 3130 Genetic Analyzer capillary sequencer.

Growth Conditions

Synechocystis strains were maintained on solid BG-11 plates (Rippka et al., 1979) that were supplemented with 1.5% agarose, 10 μg/ mL kanamycin, 5 mM glucose, 10 μM 3-(3,4-dichlorophenyl)-1,1-dimethylurea (DCMU), and 10 mM TES/KOH pH 8.2. Liquid cultures were inoculated from these plates and grown in 100 mL BG-11 media at 30º C on a rotary shaker at 200 rpm with a light intensity of 25 μEinsteins m^{-2} s^{-1}. Growth data was obtained by inoculating liquid BG-11 at a cell density of $1*10^7$ cells/mL. Kanamycin was added to all of the liquid cultures at a final concentration of 10 μg/mL. Growth was measured by taking spectrophotometric measurements at an absorbance of 730 nm on a Cary UV 100 spectrophotometer once daily for nine days.

Oxygen Evolution Assays

Oxygen evolution assays were performed using whole cells from liquid cultures on the sixth day after inoculation. The glucose was washed out of the cultures before the oxygen assays by centrifuging at 10,000 rpm for 10 minutes in a SS-34 rotor and resuspending the cells in fresh BG-11 at least two times. Oxygen evolution rates were measured using a Hansatech Clark-type electrode at 25 ºC and a light intensity of 2500 μEinstein m^{-2} s^{-1}. Assay mixtures each contained 10 μg of chlorophyll, and 1 μM 2,5- dichloro-1,4-benzoquinone (DCBQ) as the final electron acceptor. This assay gives a measurement of PSII activity, since DCBQ accepts electrons at the Q_B level.

Photoinactivation data was collected from whole cells prepared in 10 mL aliquots of cells at 10 μg chlorophyll/mL. 1 mL aliquots of cells were exposed to a high light intensity of 5000

μEinstein m^{-2} s^{-1} white light, which caused the degradation of PSII. Every two minutes for twelve minutes (chloride-limiting media) or fourteen minutes (complete media), oxygen evolution rates were measured as described above. The $t_{1/2}$ for photoinactivation was calculated from the equation:

$$t_{1/2} = 0.693 / [\ln(N_0/N)/t]$$

N_0 = rate at time zero
N = rate at final time point
t = change in time from N_0 to N

Fluorescence Assays

A Photon Systems Instruments FL/200S dual modulation fluorometer (Brno, Czech Republic) was used to take fluorescence yield measurements. Cells to be assayed were grown in BG-11 media for five days and brought to a concentration of 6 μg chlorophyll for each sample. The appropriate amount of cells were added to a 3 mL clear plastic cuvette containing 1 mM potassium ferricyanide, 330 uM DCBQ, and brought to 3 mL with fluorescence buffer (50 mM MES-NaOH, pH 6.5, 25 mM $CaCl_2$, and 10 mM NaCl). Samples were incubated in the dark in the fluorometer for five minutes. After the dark incubation, the solution was incubated for one minute with 40 μM DCMU. This protocol measured the ability of water to be utilized as electron donor.

This method of measuring chlorophyll fluorescence was adapted from Chu et al., (1994). The fluorometer program consisted of eight saturating light flashes followed by continuous actinic illumination to measure variable fluorescence, which quantified to number of functional PSII centers when hydroxylamine was substituted for water as the electron donor. Following the five minute dark incubation, addition of DCMU and a one minute incubation, 20 mM hydroxylamine was added, followed by a twenty second dark incubation prior to taking data.

Using these conditions, we obtained a quantitative estimate of the number of PSII centers in each mutant when analyzing the variable fluorescence yield.

The relative yield was quantified with the three values from the fluorescence data, Fm (the maximum fluorescence caused by photosystem II), Fo (the initial level of fluorescence caused by phycobilisomes), and Fv (Fm-Fo), the variable fluorescence yield. Relative yield was determined by dividing the mutant value of Fv by the control value of Fv. The Δ*psb*C strain was used as a negative control. This strain lacks CP43 and fails to assemble functional PSII centers.

CHAPTER 4: RESULTS

Verification of Mutagenic Plasmids

Introduction of mutants into *Synechocystis* 6803 would not be possible unless mutagenic plasmids were created and sequenced. To create these mutagenic plasmids, plasmids pAM1 (Figure 13) and pAM3 (Figure 14) were utilized along with a procedure known as overlap extension PCR. The mutagenic plasmids were then sequenced from the 5'-flanking and 3'-flanking regions to ensure that the plasmids contain no other mutations except the desired site-directed mutations, N51A and N51D. These plasmids were used to transform the wild type *Synechocystis* 6803.

Verification of Mutant Strains

The entire *psb*V gene was sequenced along with 5'-flanking and 3'-flanking regions to ensure that the *psb*V gene contains no other mutations except the desired site-directed mutation. The mutations introduced were N51D and N51A, in which the polar asparagine amino acid at position fifty one was mutated into either a polar aspartic acid or a non-polar alanine. The mutation, N51D, was expected to be similar to the control, since the mutation will allow for hydrogen bonds between aspartic acid at position fifty one on cytochrome c-550 (cyt c-550-N51D) and arginine at position 305 on CP43 (CP43-R305). However, the mutation, N51A, was expected to be a non-functional mutation, since the mutation will not allow for hydrogen bonds between alanine at position fifty one on cytochrome c-550 (cyt c-550-N51A) and CP43-R305. The control for these experiments was the wildtype that was transformed with plasmid pAM3, yielding a non-mutated *psb*V gene with a kanamycin resistance cassette inserted at the XbaI recognition site at the end of the *psb*V gene. The control was also sequenced to verify that no other mutations were present. The primers used to create the mutants are listed in Table 3. For

variable fluorescence studies, Δ*psb*C was characterized, which has the *psb*C gene (encodes CP43 subunit) deleted.

Photoautotrophic Growth

The N51 mutants and control strains were grown photoautotrophically over a nine day period to assess the effect of each mutation on the photoautotrophic growth characteristics. All strains were grown in either complete media or chloride-limiting media to assess also the effect of chloride on the photoautotrophic growth characteristics. In complete media, both N51D and N51A mutants grew at rates comparable to the control (Figure 16). In chloride-limiting media, the N51D mutant grew at the same rate as the control; however, the N51A mutant grew at a slightly depressed rate compared to the control and N51D mutant strains (Figure 17). Under chloride-limiting conditions, the control and N51D mutant strains had a growth rate of .15 O.D. per day while the N51A mutant strain had a growth rate of .0625 O.D. per day when measured in the exponential growth phase.

Oxygen Evolution Assays

Oxygen evolution rates, for both N51 mutants and control strains, were determined in either complete (Figure 18) or chloride-limiting media (Figure 19). In both medias, the strains were allowed to grow photoautotrophically before assaying for oxygen evolution. In complete media, the oxygen evolution rates of the N51D were compared to the control and there was only a ~2% loss of rate of oxygen evolution. The N51A mutant, in complete media, exhibited a loss of ~5% when compared to the control strain. When the control and each individual mutants' mean were analyzed using a paired t-test, it was determined that the N51A mutant rate, in complete media, was statistically different from the control grown in complete media. Therefore, both the N51D mutant and the control evolved oxygen at approximately the same rate

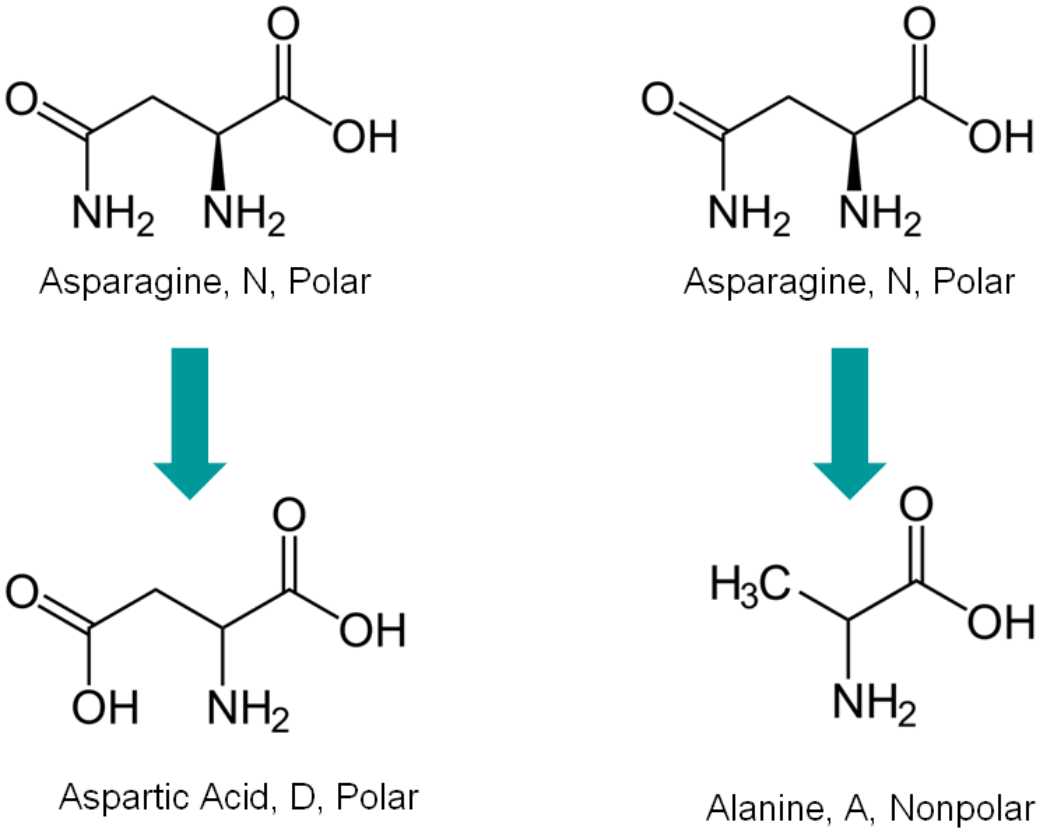

Figure 12. Site-Directed Mutagenesis was utilized to mutate the asparagine at position fifty one into either an aspartic acid (N51D) or alanine (N51A).

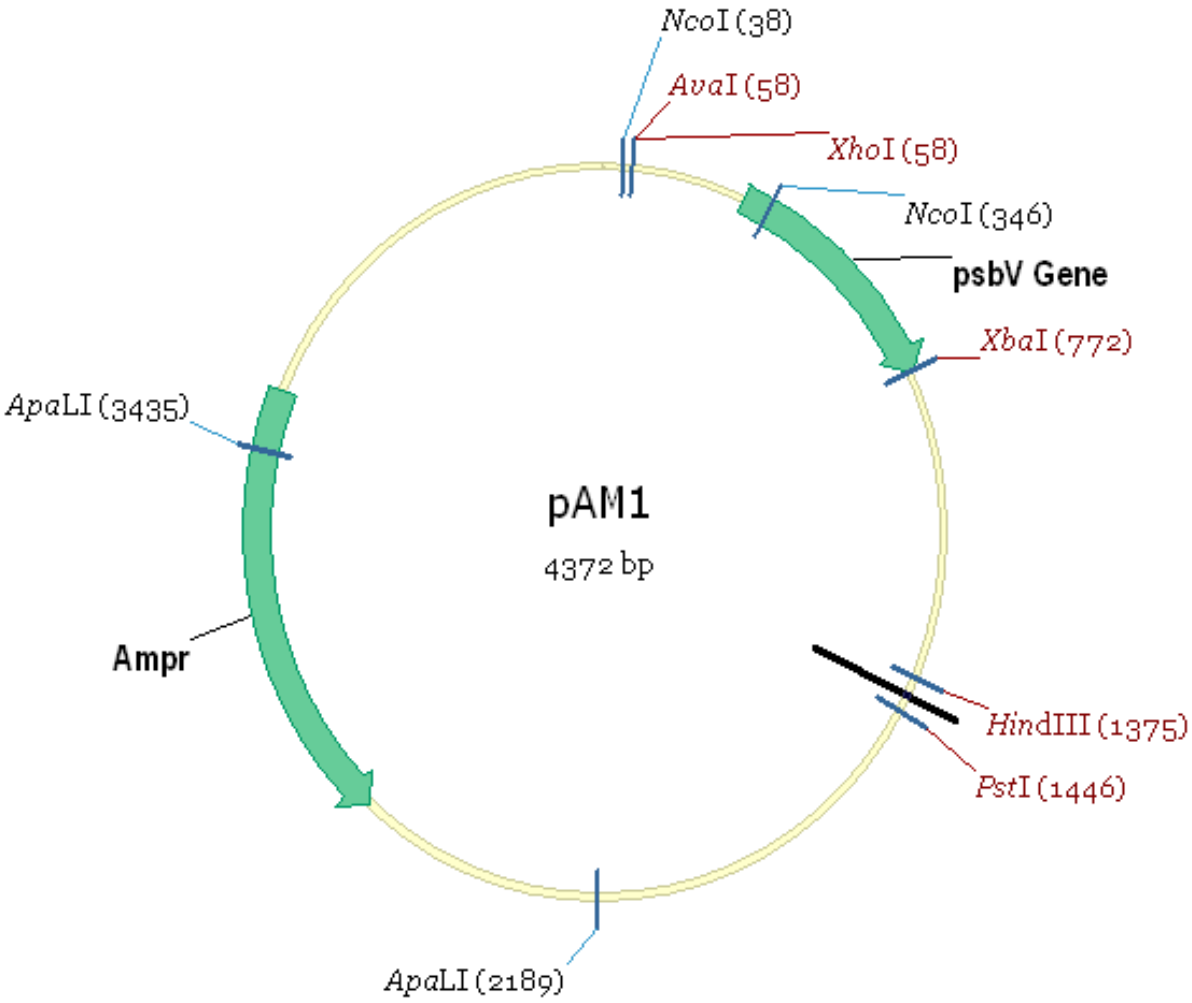

Figure 13. Plasmid pAM1 with recognition sites of a few restriction enzymes labeled, while unique recognition sites are highlighted in red.

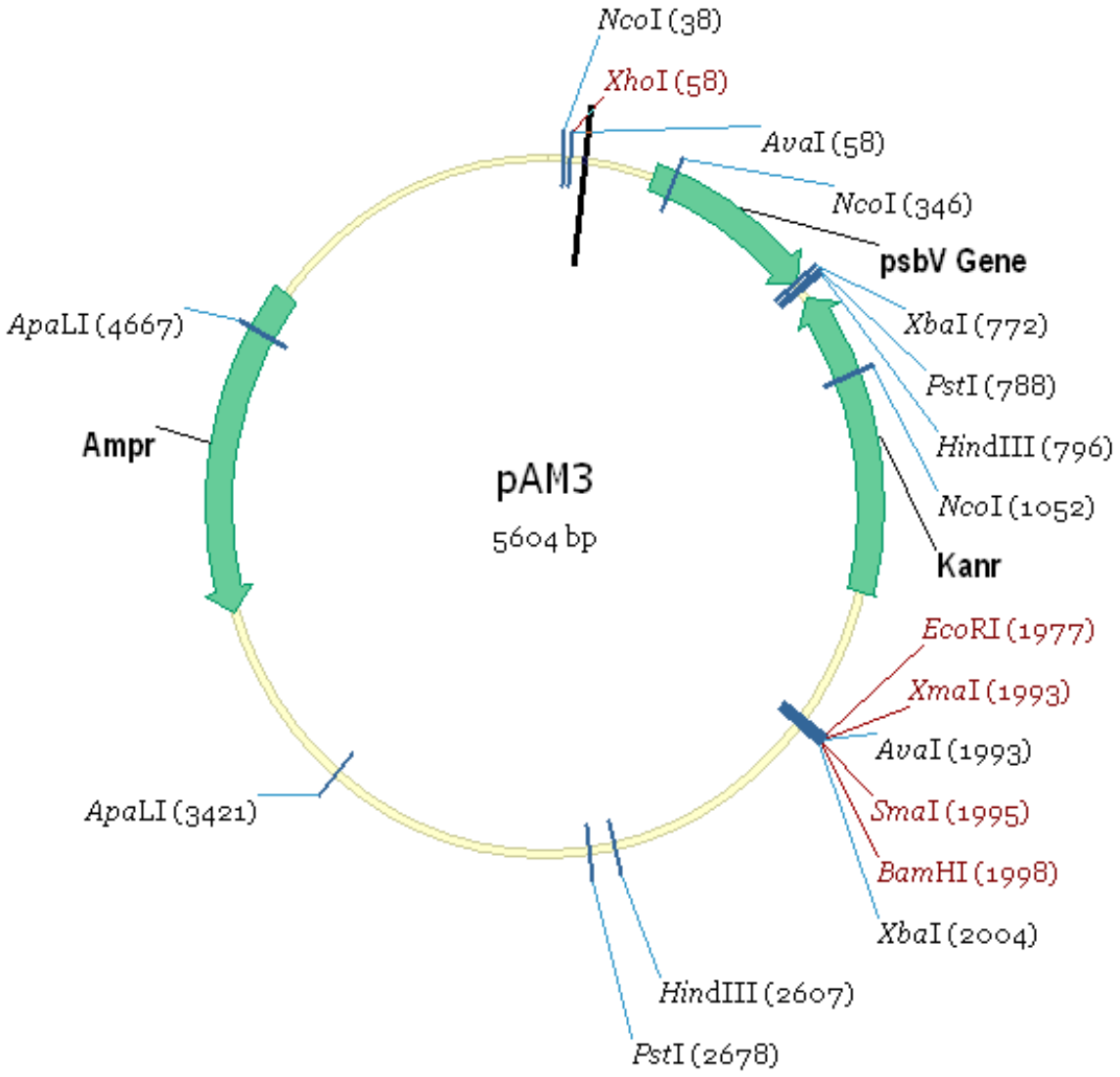

Figure 14. Plasmid pAM3 with recognition sites of a few restriction enzymes labeled, while unique recognition sites are highlighted in red.

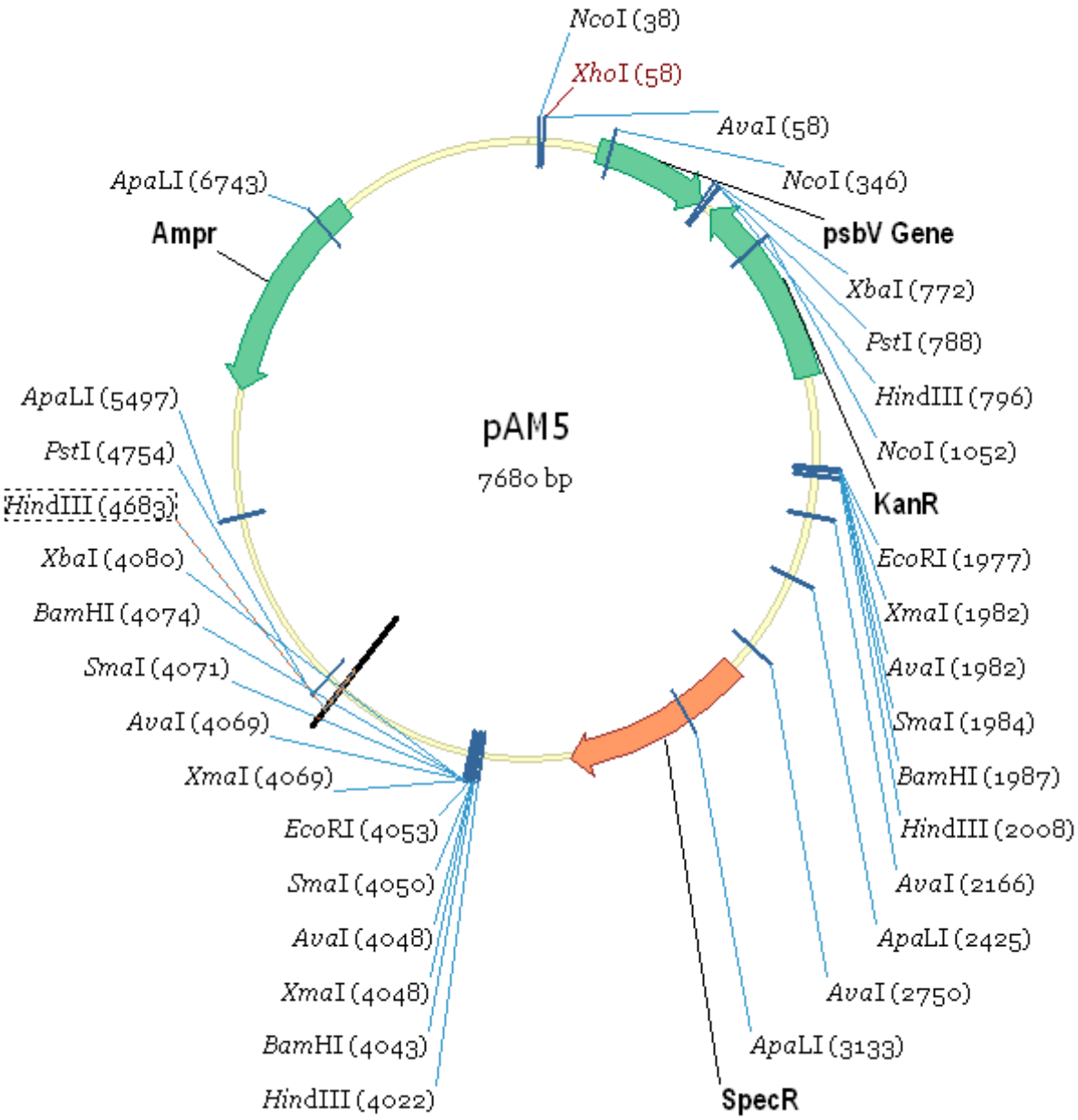

Figure 15. Plasmid pAM5 with recognition sites of a few restriction enzymes labeled, while unique recognition sites are highlighted in red.

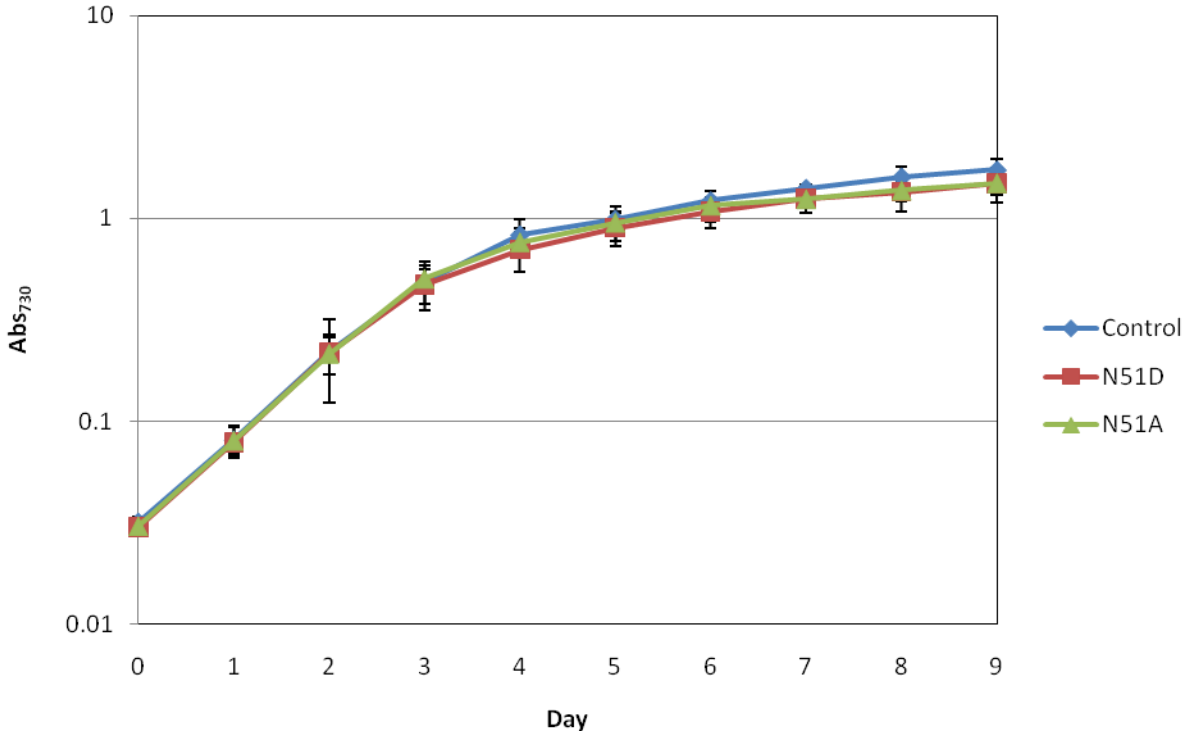

Figure 16. Photoautotrophic growth curves showing control and mutant strains grown in complete media. Each curve represents growth over nine days. The data represents the average of three independent experiments.

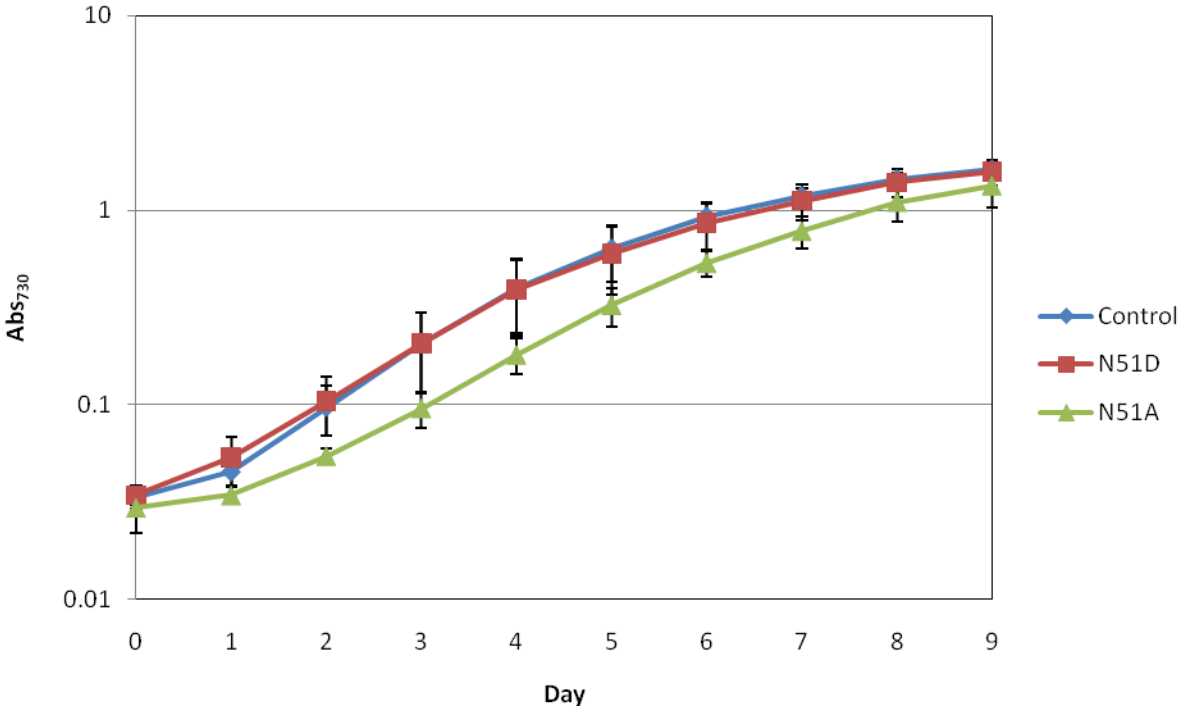

Figure 17. Photoautotrophic growth curves showing control and mutant strains grown in chloride-limiting media. Each curve represents growth over nine days. The data represents the average of three independent experiments.

in complete media while the N51A has a loss of 5% in oxygen evolution that is of statistical significance.

In chloride-limiting media, the control strain evolved oxygen at about ~87% of the rate of the control in complete media. When the N51mutant strains were compared to the control strain grown in chloride-limiting media, the N51D mutant strain showed a ~7% decreased oxygen evolution rate and the N51A mutant had a loss of ~18% in the oxygen evolution rate. However, when the N51 mutants strains were compared to the control in complete media, the N51D mutant exhibited a decrease of ~19% in the oxygen evolution rate and the N51A mutant had a decrease of 29% in the ability to evolve oxygen (compared to the 13% decrease in the oxygen evolution rate exhibited by the control). When the control grown in complete media and each individual mutants' mean, grown in chloride-limiting media, were analyzed using a paired t-test, it was determined that the N51D and N51A mutant strain are statistically different from the control grown in complete media. Therefore, both the N51D and N51A mutant strain had a loss in oxygen evolution that is of statistical significance.

Photoinactivation Assays

Photoinactivation assays can be used to determine the stability of the PSII complex of the control and mutant strains. From photoinactivation assays, the $t_{1/2}$ values of each strain can be evaluated, these values correspond to the time that oxygen evolving activity of a strain is reduced by half following the exposure to a very high light intensity; the larger the $t_{1/2}$ value, the more stable the PSII complex. Photoinactivation for both N51 mutants and the control strains were assessed in both complete (Figure 20) and chloride-limiting media (Figure 21).

In complete media, the control had a $t_{1/2}$ value of 4.9 minutes; the mutant strains have a $t_{1/2}$ value of 4.5 minutes for the N51D strain and 4.5 minutes for the N51A strain (Table 4). The

PSII centers in the N51A and N51D mutant strains seem to be equally stable in complete media. In chloride-limiting media, the control had a $t_{1/2}$ value of 6.0 minutes; the mutant strains have a $t_{1/2}$ value of 5.9 minutes for the N51D strain and 4.6 minutes for the N51A strain. In chloride-limiting conditions, the N51A mutant strain has a lower $t_{1/2}$ value than either N51D or control strains, indicating that the PSII complexes in the N51A mutant strain may be slightly more unstable than those in the control or the N51D strain.

Variable Fluorescence Yield Assays

Using variable fluorescence yield assays, the relative number of PSII centers can be estimated for each strain. Variable fluorescence yield assays also provides information on functionality of these centers. When hydroxylamine replaces the OEC as the electron donor, this technique gives an estimate of the number of PSII centers present, assuming normal electron transport between tryosine Z and Q_a. When water is used as the electron donor, this technique assesses how well water is utilized as the electron donor and thus gives information on the functioning of the manganese cluster. The results of these assays are shown in Tables 5 and 6. Both the N51 mutants and control strains were grown in either complete or chloride-limiting media.

Under either set of growth conditions, both the mutant and control strains appear to assemble high numbers of PSII centers and these centers are capable of oxidizing water. Based on paired student's t-tests, when the control was compared to the mutant strains, there was no statistical significance indicating that the all mutant and control strains accumulate the same number of PSII centers. Also, based on the same statistical modeling, there was no significance when either water or hydroxylamine was used as the electron donor. The *psb*C deletion strain, which assembles essentially no functional PSII centers, exhibited drastically decreased

fluorescence yields. These results are consistent with the results of oxygen evolution assays which exhibited high oxygen evolution rates. It should be kept in mind that, since a number of factors can affect the fluorescence yield, that these results are qualitative in nature. However, they clearly show that PSII assembly has not been affected in the mutants and that the mutants each contain a functional manganese cluster.

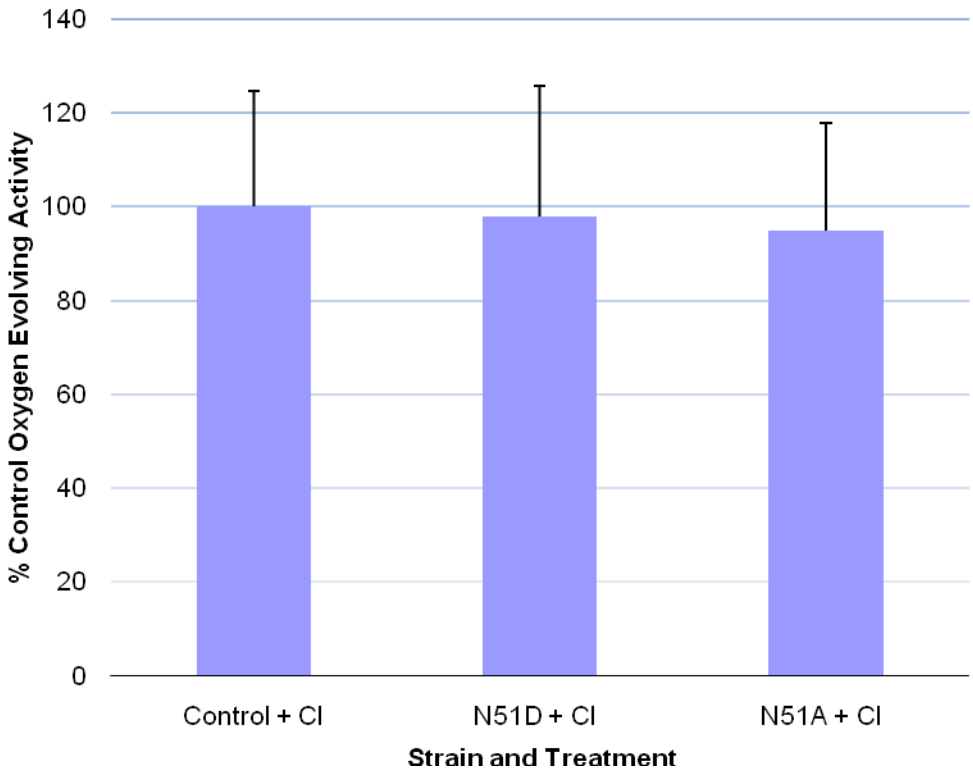

Figure 18. Oxygen evolution rates of N51 mutants and control strains grown under photoautotrophic conditions in complete media without glucose. The data represents the average of three independent experiments.

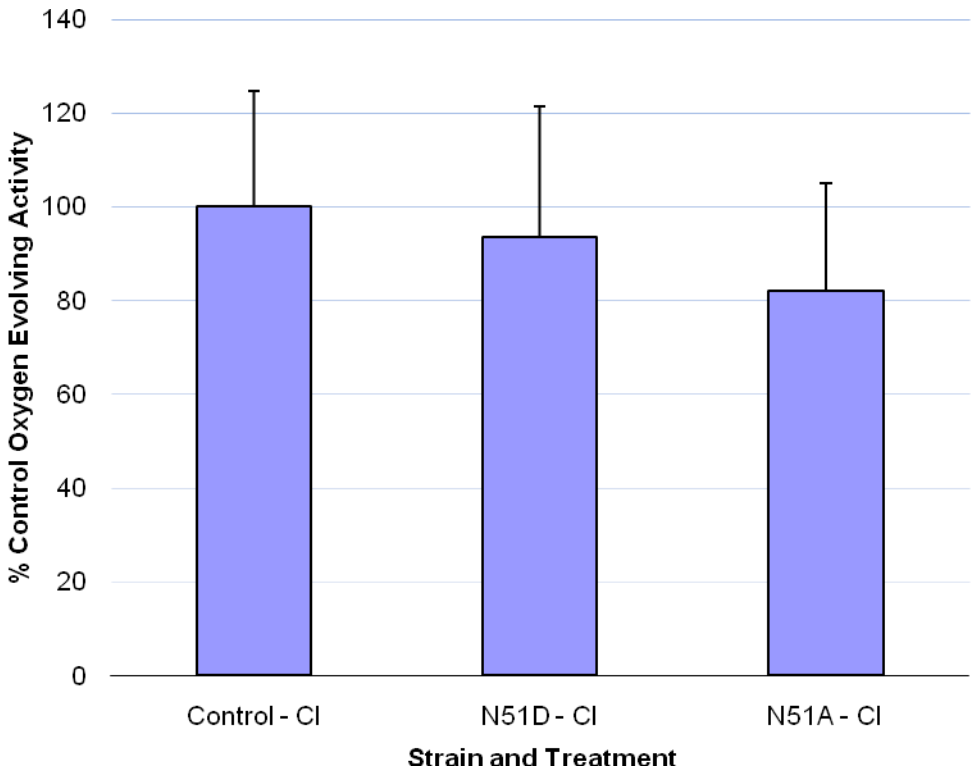

Figure 19. Oxygen evolution rates of N51 mutants and control strains grown under photoautotrophic conditions in chloride-limiting media without glucose. The data represents the average of three independent experiments.

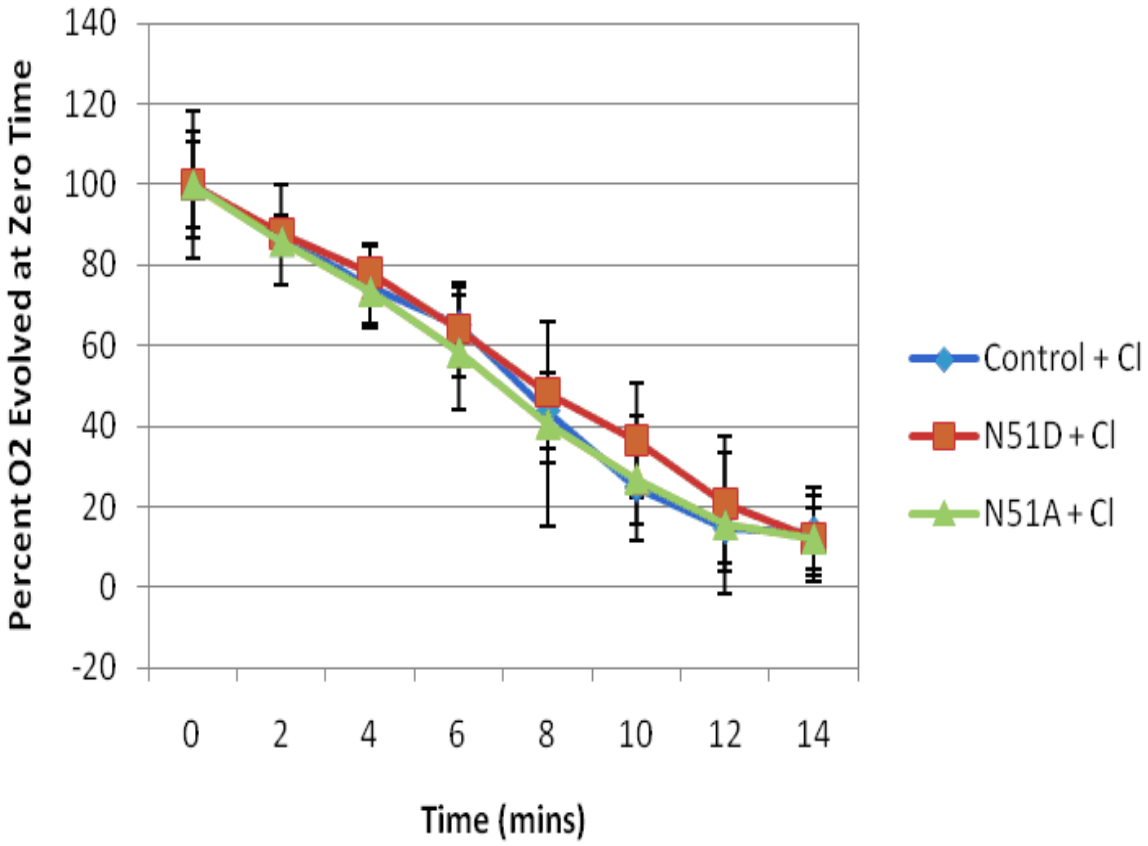

Figure 20. Photoinactivation of N51mutants and control. Cells were assayed for oxygen evolution activity every two minutes for fourteen minutes following exposure to 5000 µEinstein m^{-2} s^{-1} white light in complete media without glucose. The data represents the average of three independent experiments.

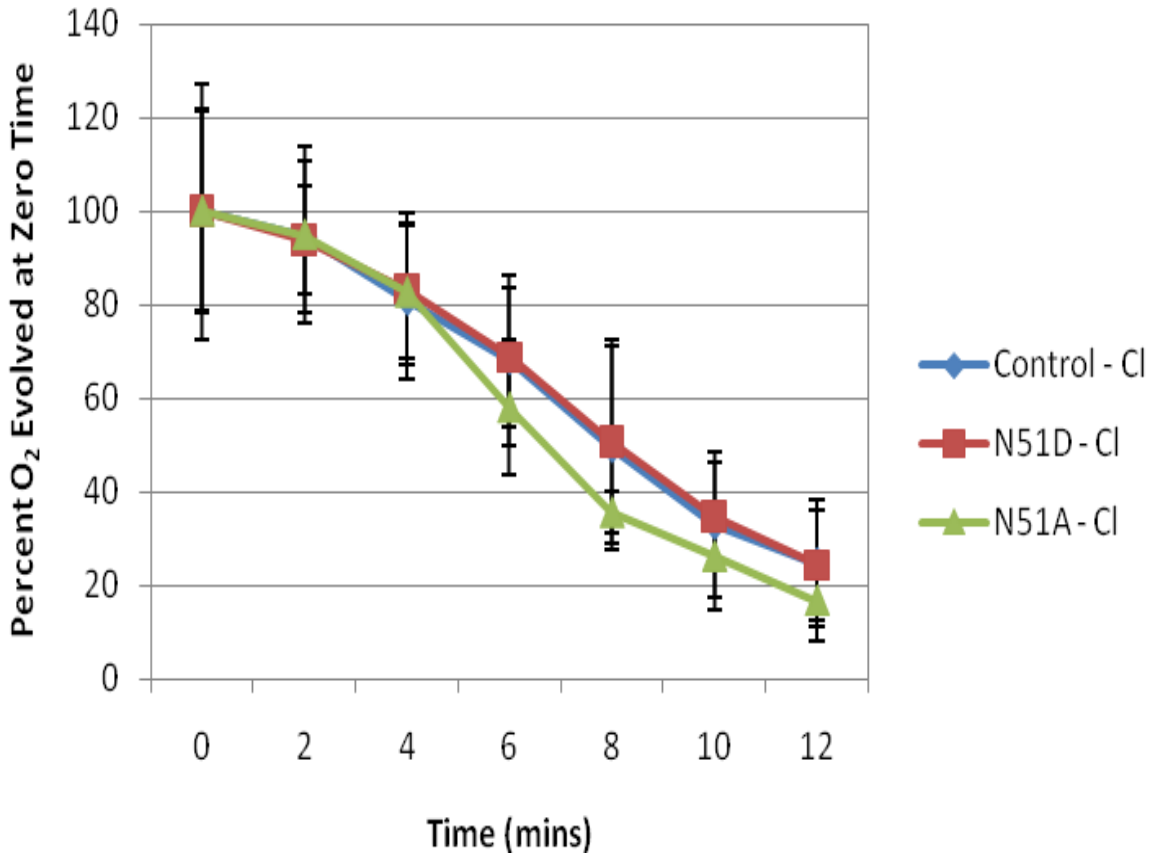

Figure 21. Photoinactivation of N51mutants and control. Cells were assayed for oxygen evolution activity every two minutes for twelve minutes following exposure to 5000 µEinstein m^{-2} s^{-1} white light in chloride-limiting media without glucose. The data represents the average of three independent experiments.

Table 4. Photoinactivation $t_{1/2}$ values for N51 mutants and control grown in complete and chloride-limiting media was calculated for fourteen minutes for complete media and twelve minutes for chloride-limiting media.

Strain	Complete Media	Chloride-Limiting Media
Control	4.9	6.0
N51D	4.5	5.9
N51A	4.5	4.6

Table 5. Results of variable fluorescence yield assays performed on control, *psbC* deletion, and N51 mutant strains in complete media. The data represents the average of three independent experiments.

Strain	Water	% Control	Standard Deviation	Hydroxylamine	% Control	Standard Deviation
*psb*C Deletion	.056	22	.003	.059	21	.005
Control	.254	100	.017	.282	100	.030
N51D	.241	95	.012	.287	102	.016
N51A	.222	87	.013	.267	95	.022

Table 6. Results of variable fluorescence yield assays performed on control, *psbC* deletion, and N51 mutant strains in chloride-limiting media. The data represents the average of three independent experiments.

Strain	Water	% Control	Standard Deviation	Hydroxylamine	% Control	Standard Deviation
*psb*C Deletion	.056	22	.003	.059	20	.005
Control - Cl	.255	100	.030	.289	100	.014
N51D - Cl	.252	99	.003	.286	99	.010
N51A - Cl	.238	93	.031	.304	105	.012

CHAPTER 5: DISCUSSION

The loss of cyt c-550 due to a mutation of arginine at position 305 in CP43 subunit to a serine residue in *Synechocystis* has been described by our lab (Bricker et al., 2002). The R305S mutant and control grew at similar rates, photoautotrophically, in complete media; however, the R305S mutant failed to grow photoautotrophically in chloride-limiting media. The R305S mutant evolved diatomic oxygen at a decreased rate of ~60% of control in complete media and evolved diatomic oxygen at a decreased rate of ~20% of control rates in chloride-limiting media. Based on photoinactivation experiments the $t_{1/2}$ value for photoinactivation for the control cells was 10 minutes for both complete and chloride-limiting media, in contrast to the $t_{1/2}$ value of 4.7 minutes for the R305S mutant in complete media and $t_{1/2}$ value of 2.6 minutes for the R305S mutant under chloride-limiting media (Young et al., 2002). These results show that under normal growth conditions, the PSII centers in the R305S mutant exhibit a modest decrease in PSII function, but this effect is greatly exacerbated under conditions of chloride depletion.

Further analysis of R305 of subunit CP43 was undertaken by mutating the arginine residue to either a lysine or an aspartic acid. The R305K mutant, R305D mutant and the control grew at similar rates, photoautotrophically, in complete media; In chloride-limiting media, the R305D mutant failed to grow at all photoautotrophically, while the R305K mutant grew at a slightly depressed rate. Oxygen evolution rates of the R305K mutant, when grown photoautotrophically in complete media, were ~80% of the control rates and ~35% of control rates in chloride-limiting media. Oxygen evolution rates of the R305D mutant, when grown photoautotrophically in complete media, were ~70% of the control rates and ~20% of control rates in chloride-limiting media. Based on photoinactivation experiments, the $t_{1/2}$ value for photoinactivation for control cells was 5.4 minutes in complete media and 5.7 minutes in

chloride-limiting media, in contrast to the $t_{1/2}$ value of 5.3 minutes for the R305K mutant in complete media and $t_{1/2}$ value of 2.9 minutes for the R305K mutant under chloride-limiting media. The R305D mutant's $t_{1/2}$ value when assayed in complete media was 3.6 minutes and 0.9 minutes in chloride-limiting media (Burch, 2003).

Based on the previous characterizations, the mutations can be ranked from having the most effect on photoautotrophic growth and oxygen evolving activity to the least effect in chloride-limiting media: R305D > R305S > R305K. The R305S and R305D mutants were more susceptible to photoinactivation than the control, indicating that these mutations decreased the stability of the PSII complex. Substitution of arginine by the like charged amino acid lysine resulted in a mutant exhibiting fairly normal PSII activity. Therefore, it was concluded that a positive charge is required at position 305 on CP43.

The above studies predicted a charge-charge (electrostatic) interaction between CP43 and cyt c-550. However, based on current x-ray structures of PSII, the region of cyt c-550 that is most probably interacting with R305-CP43 does not have any charged (positive or negative) amino acids in the vicinity of R305. This study investigates the interaction between CP43 and cyt c-550 by identifying amino acids that might be involved in this interaction and mutating these amino acids. Based on x-ray structure of PSII, two amino acids on cyt c-550 were identified as potential candidates for mutagenesis based solely on their close proximity to R305-CP43 (Loll et al., 2005). The two amino acids are highly conserved asparagines at position forty-nine (2.76 Å from R305-CP43) and fifty-one (3.729 Å from R305-CP43). In this study, the asparagine residue at position fifty-one on cyt c-550 was mutated to either an alanine or aspartic acid residue. In twelve different species used to create the alignment sequences in Figure 10, only one organism does not conserve asparagine at position fifty-one; that organism is

cyanobacterium *Thermosynechoccus elongatus*, the organism from which the x-ray structures are derived. The distance between serine at position fifty-one of cyt c-550 and arginine at position 305 of CP43 is 3.729 Å. Since this amino acid is asparagine in our model organism, *Synechocystis* 6803, we cannot definitively quantify the distance of the side chain to the arginine on CP43. It should be noted that we attempted to construct the corresponding mutations at position N49. While we were successful in producing mutant plasmids, these failed to transform *Synechocystis*.

Based on the observed results, N51-cyt c-550 may contribute to a weak interaction between CP43 and cyt c-550. The N51A mutant has an overall small but consistent effect on photoautotrophic growth, oxygen evolution rates and photoinactivation $t_{1/2}$ values in chloride-limiting media, but exhibits a phenotype identical to the control in complete media. Since the extrinsic proteins aid in retaining calcium and chloride ions, if the N51A mutation resulted in a decrease affinity of cyt c-550 to CP43, then we would expect that only in chloride-limiting media would a resulting phenotype be observable. The N51D mutant phenotype in all assays produced results that were identical to the control in both chloride-limiting and complete media.

A new proposal for the interaction between cyt c-550 and CP43 based on the current characterization involves two criteria: hydrogen bonds and the length between the relevant amino acid side chains. The proposed interaction involves hydrogen bonds forming between the asparagine residues at positions forty-nine and fifty-one of cyt c-550 and the arginine residue of CP43. The electronegative atoms on asparagine and arginine are highly susceptible to hydrogen bonding. In addition, the length of the side chain at position 305 of CP43 needs to be sufficient to reach the asparagine residues on cyt c-550 as indicated also by previous characterization studies (Burch, 2003). The distance between the electronegative atoms on R305-CP43 and N49-

cyt c-550 and N51-cyt c-550 also supports hydrogen bonding and why the length of the amino acids at these positions are so important. The distances from the electronegative atom, covalently bonded to the hydrogen, to the electronegative atom forming the hydrogen bond have a range from 2.7 Å to 3.1 Å . Since the N51D mutation conserves the electronegative atoms it might be involved in hydrogen bonding, as distinct phenotype was not observed.

This model can be extrapolated to discuss previous mutations of R305-CP43, in which mutations were ranked from having the most effect on photoautotrophic growth and oxygen evolving activity to the least effect in chloride-limiting media: R305D > R305S > R305K. The R305K mutation resulted in the least effect in chloride-limiting media because lysine can also form hydrogen bonds, but has only one electronegative nitrogen instead of the three electronegative nitrogens present on arginine. Both, R305D and R305S may lack the length to reach cyt c-550 and thus had the most severe effect on photoautotrophic growth and oxygen evolving activity.

There are other possibilities to explain the phenotype of the N51A mutant. It could be that N49-cyt c-550 constitutes a larger portion of the interactions between CP43 and cyt c-550 while N51-cyt c-550 constitutes only a small portion of the interaction. This is why construction of an N49 mutant is particularly important. Alanine cannot form hydrogen bonds via its side chain. However, it is possible that arginine 305 on CP43 might be forming hydrogen bonds to N51A via its carbonyl backbone; and this could explain the observed modest phenotype (Borders et al., 1994). Arginine can form a maximum of five hydrogen bonds; other amino acids in cyt. c-550 or other PSII proteins may be H-bond partners and the disruption of a single one of these may not be disruptive enough to produce a severe phenotype. When cyt c-550 is isolated in its monomeric and dimeric form, the carbonyl groups on the backbone of the β-turn are

oriented towards the heme, stabilizing the oxidized state. Cyt c-550 bound to PSII repositions the carbonyl groups, and R305-CP43 might enforce the reorientation of the backbone carbonyl groups (Ishikita and Knapp, 2005).

The effect of the N51A mutant's phenotype might also be due to the change in topology arising due to the mutation from an asparagine to an alanine and not due to the loss of hydrogen bonding between CP43 and cyt c-550.

Further studies are needed to validate the proposed interaction between subunits cyt c-550 and CP43 of PSII.

CHAPTER 6: REFERENCES

Alexeyev, M.F. (1995). Three kanamycin resistance gene cassettes with different polylinkers. BioTechniques *18,* 52, 54, 56.

Andrews, H., Li, Z., Altuve-Blanco, A., Rivera, M., and Burnap, R.L. (2005). Expression, mutagenesis, and characterization of recombinant low-potential cytochrome c550 of photosystem II. Biochemistry *44,* 6092-6100.

Barber, J., and Murray W. James. (2008). Revealing the structure of the Mn-cluster of photosystem II by X-ray crystallography. Coordination Chemistry Reviews *252,* 233.

Bienert, R., Rombach-Riegraf, V., Diez, M., and Graber, P. (2009). Subunit movements in single membrane-bound H+-ATP synthases from chloroplasts during ATP synthesis. J. Biol. Chem. *284,* 36240-36247.

Borders, C.L.,Jr, Broadwater, J.A., Bekeny, P.A., Salmon, J.E., Lee, A.S., Eldridge, A.M., and Pett, V.B. (1994). A structural role for arginine in proteins: multiple hydrogen bonds to backbone carbonyl oxygens. Protein Sci. *3,* 541-548.

Brandon Douglas Burch. (2003). Characterization of the effects of chloride depletion on oxygen evolving activity in the R305D and R305K mutants of the CP43 protein of photosystem II.

Breyton, C. (2000). The cytochrome b(6)f complex: structural studies and comparison with the bc(1) complex. Biochim. Biophys. Acta *1459,* 467-474.

Bricker, T.M., Young, A., Frankel, L.K., and Putnam-Evans, C. (2002). Introduction of the 305Arg-->305Ser mutation in the large extrinsic loop E of the CP43 protein of *Synechocystis* sp. PCC 6803 leads to the loss of cytochrome c(550) binding to Photosystem II. Biochim. Biophys. Acta *1556,* 92-96.

Brudvig, G.W. (2008). Water oxidation chemistry of photosystem II. Philos. Trans. R. Soc. Lond. B. Biol. Sci. *363,* 1211-8; discussion 1218-9.

Campbell, D., Hurry, V., Clarke, A.K., Gustafsson, P., and Oquist, G. (1998). Chlorophyll fluorescence analysis of cyanobacterial photosynthesis and acclimation. Microbiol. Mol. Biol. Rev. *62,* 667-683.

Chu, H.A., Nguyen, A.P., and Debus, R.J. (1994). Site-directed photosystem II mutants with perturbed oxygen-evolving properties. 1. Instability or inefficient assembly of the manganese cluster in vivo. Biochemistry *33,* 6137-6149.

Chu, H.A., Nguyen, A.P., and Debus, R.J. (1994). Site-directed photosystem II mutants with perturbed oxygen-evolving properties. 1. Instability or inefficient assembly of the manganese cluster in vivo. Biochemistry *33,* 6137-6149.

Clarke, S.M., and Eaton-Rye, J.J. (2000). Amino acid deletions in loop C of the chlorophyll a-binding protein CP47 alter the chloride requirement and/or prevent the assembly of photosystem II. Plant Mol. Biol. *44,* 591-601.

Cramer, W.A., and Zhang, H. (2006). Consequences of the structure of the cytochrome b6f complex for its charge transfer pathways. Biochimica Et Biophysica Acta (BBA) - Bioenergetics *1757,* 339-345.

Debus, R.J. (2008). Protein Ligation of the Photosynthetic Oxygen-Evolving Center. Coord. Chem. Rev. *252,* 244-258.

Debus, R.J., Barry, B.A., Sithole, I., Babcock, G.T., and McIntosh, L. (1988). Directed mutagenesis indicates that the donor to P+680 in photosystem II is tyrosine-161 of the D1 polypeptide. Biochemistry *27,* 9071-9074.

Debus, R.J., Strickler, M.A., Walker, L.M., and Hillier, W. (2005). No evidence from FTIR difference spectroscopy that aspartate-170 of the D1 polypeptide ligates a manganese ion that undergoes oxidation during the S0 to S1, S1 to S2, or S2 to S3 transitions in photosystem II. Biochemistry *44,* 1367-1374.

Enami, I., Okumura, A., Nagao, R., Suzuki, T., Iwai, M., and Shen, J.R. (2008). Structures and functions of the extrinsic proteins of photosystem II from different species. Photosynth Res. *98,* 349-363.

Ferreira, K.N., Iverson, T.M., Maghlaoui, K., Barber, J., and Iwata, S. (2004). Architecture of the photosynthetic oxygen-evolving center. Science *303,* 1831-1838.

Guskov, A., Kern, J., Gabdulkhakov, A., Broser, M., Zouni, A., and Saenger, W. (2009). Cyanobacterial photosystem II at 2.9-A resolution and the role of quinones, lipids, channels and chloride. Nat. Struct. Mol. Biol. *16,* 334-342.

Han, K.C., Shen, J.R., Ikeuchi, M., and Inoue, Y. (1994). Chemical crosslinking studies of extrinsic proteins in cyanobacterial photosystem II. FEBS Lett. *355,* 121-124.

Haumann, M., Barra, M., Loja, P., Loscher, S., Krivanek, R., Grundmeier, A., Andreasson, L.E., and Dau, H. (2006). Bromide does not bind to the Mn4Ca complex in its S1 state in Cl(-)-depleted and Br(-)-reconstituted oxygen-evolving photosystem II: evidence from X-ray absorption spectroscopy at the Br K-edge. Biochemistry *45,* 13101-13107.

Haumann, M., Liebisch, P., Muller, C., Barra, M., Grabolle, M., and Dau, H. (2005). Photosynthetic O2 formation tracked by time-resolved x-ray experiments. Science *310,* 1019-1021.

Heckman, K.L., and Pease, L.R. (2007). Gene splicing and mutagenesis by PCR-driven overlap extension. Nat. Protoc. *2,* 924-932.

Hendry, G., and Wydrzynski, T. (2003). (18)O isotope exchange measurements reveal that calcium is involved in the binding of one substrate-water molecule to the oxygen-evolving complex in photosystem II. Biochemistry *42,* 6209-6217.

Hwang, H.J., Dilbeck, P., Debus, R.J., and Burnap, R.L. (2007). Mutation of arginine 357 of the CP43 protein of photosystem II severely impairs the catalytic S-state cycle of the H2O oxidation complex. Biochemistry *46,* 11987-11997.

Ishikita, H., and Knapp, E.W. (2005). Redox potential of cytochrome c550 in the cyanobacterium Thermosynechococcus elongates. FEBS Lett. *579,* 3190-3194.

Joliot, P. (1968). Kinetic studies of photosystem II in photosynthesis. Photochem. Photobiol. *8,* 451-463.

Kang, C., Chitnis, P.R., Smith, S., and Krogmann, D.W. (1994). Cloning and sequence analysis of the gene encoding the low potential cytochrome c of *Synechocystis* PCC 6803. FEBS Lett. *344,* 5-9.

Kawakami, K., Umena, Y., Kamiya, N., and Shen, J.R. (2009). Location of chloride and its possible functions in oxygen-evolving photosystem II revealed by X-ray crystallography. Proc. Natl. Acad. Sci. U. S. A. *106,* 8567-8572.

Kerfeld, C.A., Sawaya, M.R., Bottin, H., Tran, K.T., Sugiura, M., Cascio, D., Desbois, A., Yeates, T.O., Kirilovsky, D., and Boussac, A. (2003). Structural and EPR characterization of the soluble form of cytochrome c-550 and of the *psb*V2 gene product from the cyanobacterium Thermosynechococcus elongatus. Plant Cell Physiol. *44,* 697-706.

Knoepfle, N., Bricker, T.M., and Putnam-Evans, C. (1999). Site-directed mutagenesis of basic arginine residues 305 and 342 in the CP 43 protein of photosystem II affects oxygen-evolving activity in *Synechocystis* 6803. Biochemistry *38,* 1582-1588.

Kok, B., Forbush, B., and McGloin, M. (1970). Cooperation of charges in photosynthetic O2 evolution-I. A linear four step mechanism. Photochem. Photobiol. *11,* 457-475.

Kufryk, G.I., Sachet, M., Schmetterer, G., and Vermaas, W.F. (2002). Transformation of the cyanobacterium *Synechocystis* sp. PCC 6803 as a tool for genetic mapping: optimization of efficiency. FEMS Microbiol. Lett. *206,* 215-219.

Lee, C.I., Lakshmi, K.V., and Brudvig, G.W. (2007). Probing the functional role of Ca2+ in the oxygen-evolving complex of photosystem II by metal ion inhibition. Biochemistry *46,* 3211-3223.

Li, Z., Andrews, H., Eaton-Rye, J.J., and Burnap, R.L. (2004). In situ effects of mutations of the extrinsic cytochrome c550 of photosystem II in *Synechocystis* sp. PCC6803. Biochemistry *43,* 14161-14170.

Lindberg, K., and Andreasson, L.E. (1996). A one-site, two-state model for the binding of anions in photosystem II. Biochemistry *35*, 14259-14267.

Liu, L., Chen, X., Zhang, Y., and Zhou, B. (2005). Characterization, structure and function of linker polypeptides in phycobilisomes of cyanobacteria and red algae: An overview. Biochimica Et Biophysica Acta (BBA) - Bioenergetics *1708*, 133-142.

Loll, B., Kern, J., Saenger, W., Zouni, A., and Biesiadka, J. (2005). Towards complete cofactor arrangement in the 3.0 A resolution structure of photosystem II. Nature *438*, 1040-1044.

Manna, P., and Vermaas, W. (1997). Mutational studies on conserved histidine residues in the chlorophyll-binding protein CP43 of photosystem II. Eur. J. Biochem. *247*, 666-672.

Mao, J., Hauser, K., and Gunner, M.R. (2003). How cytochromes with different folds control heme redox potentials. Biochemistry *42*, 9829-9840.

Medina, M. (2009). Structural and mechanistic aspects of flavoproteins: photosynthetic electron transfer from photosystem I to NADP+. FEBS J. *276*, 3942-3958.

Miqyass, M., van Gorkom, H.J., and Yocum, C.F. (2007). The PSII calcium site revisited. Photosynth Res. *92*, 275-287.

Mohanty, P., Allakhverdiev, S.I., and Murata, N. (2007). Application of low temperatures during photoinhibition allows characterization of individual steps in photodamage and the repair of photosystem II. Photosynth Res. *94*, 217-224.

Nelson, N., and Yocum, C.F. (2006). STRUCTURE AND FUNCTION OF PHOTOSYSTEMS I AND II. Annual Review of Plant Biology *57*, 521-565.

Nishiyama, Y., Allakhverdiev, S.I., and Murata, N. (2005). Inhibition of the repair of photosystem II by oxidative stress in cyanobacteria. Photosynth Res. *84*, 1-7.

Olesen, K., and Andreasson, L.E. (2003). The function of the chloride ion in photosynthetic oxygen evolution. Biochemistry *42*, 2025-2035.

Pakrasi, H.B., Diner, B.A., Williams, J., and Arntzen, C.J. (1989). Deletion Mutagenesis of the Cytochrome b559 Protein Inactivates the Reaction Center of Photosystem II. Plant Cell *1*, 591-597.

Popelkova, H., and Yocum, C.F. (2007). Current status of the role of Cl(-) ion in the oxygen-evolving complex. Photosynth Res. *93*, 111-121.

Rippka, R., Derueles, J., Waterbury, J.B., and Herdman, M.S., R.Y. (1979). Generic assignments, strain histories and properties of pure cultures of Cyanobacteria. J Gen Microbiol *111*, 1.

Roose, J.L., Kashino, Y., and Pakrasi, H.B. (2007). The PsbQ protein defines cyanobacterial Photosystem II complexes with highest activity and stability. Proc. Natl. Acad. Sci. U. S. A. *104*, 2548-2553.

Roose, J.L., Wegener, K.M., and Pakrasi, H.B. (2007). The extrinsic proteins of Photosystem II. Photosynth Res. *92*, 369-387.

Rosenberg, C., Christian, J., Bricker, T.M., and Putnam-Evans, C. (1999). Site-directed mutagenesis of glutamate residues in the large extrinsic loop of the photosystem II protein CP 43 affects oxygen-evolving activity and PS II assembly. Biochemistry *38*, 15994-16000.

Shen, J.R., Qian, M., Inoue, Y., and Burnap, R.L. (1998). Functional characterization of *Synechocystis* sp. PCC 6803 delta *psb*U and delta *psb*V mutants reveals important roles of cytochrome c-550 in cyanobacterial oxygen evolution. Biochemistry *37*, 1551-1558.

Shen, J.R., Vermaas, W., and Inoue, Y. (1995). The role of cytochrome c-550 as studied through reverse genetics and mutant characterization in *Synechocystis* sp. PCC 6803. J. Biol. Chem. *270*, 6901-6907.

Shimada, Y., Suzuki, H., Tsuchiya, T., Tomo, T., Noguchi, T., and Mimuro, M. (2009). Effect of a single-amino acid substitution of the 43 kDa chlorophyll protein on the oxygen-evolving reaction of the cyanobacterium *Synechocystis* sp. PCC 6803: analysis of the Glu354Gln mutation. Biochemistry *48*, 6095-6103.

Tagore, R., Chen, H., Crabtree, R.H., and Brudvig, G.W. (2006). Determination of mu-oxo exchange rates in di-mu-oxo dimanganese complexes by electrospray ionization mass spectrometry. J. Am. Chem. Soc. *128*, 9457-9465.

Tagore, R., Crabtree, R.H., and Brudvig, G.W. (2007). Distinct mechanisms of bridging-oxo exchange in di-mu-O dimanganese complexes with and without water-binding sites: implications for water binding in the O(2)-evolving complex of photosystem II. Inorg. Chem. *46*, 2193-2203.

Terry M. Bricker, and Robert L. Burnap. (2005). The extrinsic Protiens of Photosystem II. In Photosystem II The Light-Driven Water:Plastoquinone Oxidoreductase, Thomas J. Wydrzynski, and Kimiyuki Satoh eds., Springer) pp. 95.

Vrettos, J.S., and Brudvig, G.W. (2002). Water oxidation chemistry of photosystem II. Philos. Trans. R. Soc. Lond. B. Biol. Sci. *357*, 1395-404; discussion 1404-5, 1419-20.

Vrettos, J.S., Reifler, M.J., Kievit, O., Lakshmi, K.V., de Paula, J.C., and Brudvig, G.W. (2001). Factors that determine the unusually low reduction potential of cytochrome c550 in cyanobacterial photosystem II. J. Biol. Inorg. Chem. *6*, 708-716.

Wydrzynski, T.J. (2008). Water splitting by Photosystem II--where do we go from here? Photosynth Res. *98*, 43-51.

Yano, J., Kern, J., Irrgang, K.D., Latimer, M.J., Bergmann, U., Glatzel, P., Pushkar, Y., Biesiadka, J., Loll, B., Sauer, K., *et al.* (2005). X-ray damage to the Mn4Ca complex in single crystals of photosystem II: a case study for metalloprotein crystallography. Proc. Natl. Acad. Sci. U. S. A. *102*, 12047-12052.

Yano, J., Kern, J., Sauer, K., Latimer, M.J., Pushkar, Y., Biesiadka, J., Loll, B., Saenger, W., Messinger, J., Zouni, A., and Yachandra, V.K. (2006). Where water is oxidized to dioxygen: structure of the photosynthetic Mn4Ca cluster. Science *314*, 821-825.

Young, A., McChargue, M., Frankel, L.K., Bricker, T.M., and Putnam-Evans, C. (2002). Alterations of the oxygen-evolving apparatus induced by a 305Arg --> 305Ser mutation in the CP43 protein of photosystem II from *Synechocystis* sp. PCC 6803 under chloride-limiting conditions. Biochemistry *41*, 15747-15753.